

The Inverse Gamma-Gamma Prior for Optimal Posterior Contraction and Multiple Hypothesis Testing ^{*}

Ray Bai
Malay Ghosh [†]

University of Florida

July 6, 2022

Abstract

We study the well-known problem of estimating a sparse n -dimensional unknown mean vector $\boldsymbol{\theta} = (\theta_1, \dots, \theta_n)$ with entries corrupted by Gaussian white noise. In the Bayesian framework, continuous shrinkage priors which can be expressed as scale-mixture normal densities are popular for obtaining sparse estimates of $\boldsymbol{\theta}$. In this article, we introduce a new fully Bayesian scale-mixture prior known as the inverse gamma-gamma (IGG) prior. We show that the posterior distribution contracts around the true $\boldsymbol{\theta}$ at (near) minimax rate under very mild conditions. To classify true signals ($\theta_i \neq 0$), we also propose a hypothesis test based on thresholding the posterior mean. In the context of multiple hypothesis testing, Bogdan et al. [8] introduced the notion of asymptotically Bayes optimality under sparsity (ABOS). Taking the loss function to be the expected number of misclassified tests, our test procedure asymptotically attains the ABOS risk exactly. The IGG prior appears to be the first fully Bayesian continuous shrinkage prior that both attains the minimax posterior contraction rate and that induces a multiple testing rule which is asymptotically Bayes optimal under sparsity. In addition to its theoretical guarantees, simulations show that the IGG outperforms other continuous shrinkage priors for both estimation and classification.

^{*}Keywords and phrases: normal means problem, sparsity, nearly black vectors, posterior contraction, multiple hypothesis testing, heavy tail, shrinkage estimation

[†]Malay Ghosh (email: ghoshm@ufl.edu) is Distinguished Professor, Department of Statistics, University of Florida. Ray Bai (email: raybai07@ufl.edu) is Graduate Student, Department of Statistics, University of Florida.

1 Introduction

1.1 The Normal Means Problem Revisited

Suppose we observe an n -component random observation $(X_1, \dots, X_n) \in \mathbb{R}^n$, such that

$$X_i = \theta_i + \epsilon_i, \quad i = 1, \dots, n, \quad (1)$$

where $\epsilon_i \sim N(0, 1), i = 1, \dots, n$. In the high-dimensional setting where n is very large, sparsity is a very common phenomenon. That is, in the unknown mean vector $\boldsymbol{\theta} = (\theta_1, \dots, \theta_n)$, only a few of the θ_i 's are nonzero. Under model (1), we are primarily interested in separating the signals ($\theta_i \neq 0$) from the noise ($\theta_i = 0$) and giving robust estimates of the signals.

This simple framework (1) is the basis for a number of high-dimensional problems, such as image reconstruction, genetics, and wavelet analysis (Johnstone and Silverman [21]). For example, if we wish to reconstruct an image from millions of pixels of data, only a few pixels are typically needed to recover the objects of interest. In genetics, we may have tens of thousands of gene expression data points, but only a few are significantly associated with the phenotype of interest. For instance, Wellcome Trust [33] has confirmed that only seven genes have a non-negligible association with Type I diabetes. These applications demonstrate that sparsity is a fairly reasonable assumption for $\boldsymbol{\theta}$ in (1).

1.2 Methods for Sparse Estimation of Normal Mean Vectors

Existing frequentist methods for obtaining a sparse estimate of $\boldsymbol{\theta}$ in (1) include the popular LASSO (Tibshirani [28]) and its many variants (see, for example, Zou [35], Zou and Hastie [36], Yuan and Lin [34], Tibshirani et al. [29]). All of these methods use either an ℓ_1 or a combination of an ℓ_1 and ℓ_2 penalty function to shrink many of the θ_i 's to zero. These methods are able to produce point estimates with good theoretical and empirical properties. However, in many cases, it is desirable to obtain not only a point estimate but a realistic characterization of uncertainty in the parameter estimates. In high-dimensional settings, frequentist approaches to characterizing uncertainty, such as bootstrapping or constructing confidence regions, can break down (Bhattacharya et al. [7]).

Bayesian approaches to estimating $\boldsymbol{\theta}$, on the other hand, give a natural way to quantify uncertainty through the posterior density. Spike-and-slab priors are a particularly appealing way to model sparsity. The original spike-and-slab model, introduced by Mitchell and Beauchamp [23], was of

the form,

$$\pi(\theta_i) = (1 - p)\delta_0(\theta_i) + p\psi(\theta_i|\lambda), \quad i = 1, \dots, n, \quad (2)$$

where $\delta_0(\cdot)$ is the “spike” distribution (a point mass at zero), $\psi(\cdot|\lambda)$ is an absolutely continuous “slab” distribution, indexed by a hyper-parameter λ , and p is a mixing proportion. The “spike” forces some coefficients to zero, while the “slab” models the signals.

There is a large body of theoretical evidence in favor of point-mass mixture priors (2) (for instance, see George and Foster [14], Johnstone and Silverman [21], Johnstone and Silverman [22], Castillo and van der Vaart [11], Abramovich et al. [1]). As remarked by Carvalho et al. [9], a carefully chosen “two-groups” model can be considered a “gold standard” for sparse problems. Johnstone and Silverman [21] utilized an empirical Bayes variant of (2). With a restricted marginal maximum likelihood estimate of p and a sufficiently heavy-tailed density for $\psi(\cdot|\lambda)$, they showed that the posterior mean and median both contract around the true $\boldsymbol{\theta}$ at minimax rate. They also showed that with a suitable beta prior on p , the entire posterior distribution contracts at this minimax rate. A thorough discussion of minimax estimation and contraction is deferred to Section 4.1.

Despite these desirable theoretical properties, these point-mass mixtures face computational difficulties in high dimensions since they require searching over 2^n possible models. To circumvent this problem, fully continuous variants of spike-and-slab densities have been developed. George and McCulloch [15] proposed the stochastic search variable selection (SSVS) method, which places a mixture prior of two normal densities with different variances (one small and one large) on each of the θ_i ’s. More recently, Ročková and George [26] introduced the spike-and-slab LASSO (SSL), which is a mixture of two Laplace densities with different variances (one small and one large). By specifying suitable variances for the two Laplace densities and placing an appropriate beta prior on the mixing proportion p , Ročková [25] showed that the posterior distribution of the SSL contracts at (near) minimax rate.

1.3 Scale-Mixture Shrinkage Priors

Because of the computational difficulties of (point-mass) spike-and-slab priors, a rich variety of continuous shrinkage priors which can be expressed as scale mixtures of normal densities has also been developed. These priors behave similarly to spike-and-slab priors but require significantly less computational effort. They mimic (2) in that they contain significant probability around zero so that most coefficients are shrunk to zero. However,

they retain heavy enough tails in order to correctly identify and prevent overshrinkage of the true signals. These priors typically take the form

$$\theta_i | \sigma_i^2 \sim N(0, \sigma_i^2), \quad \sigma_i^2 \sim \pi(\sigma_i^2), \quad i = 1, \dots, n, \quad (3)$$

where $\pi : [0, \infty) \rightarrow [0, \infty)$ is a density on the positive reals. π may depend on further hyperparameters, of which there may or may not be additional priors placed on them. Priors on σ_i^2 in (3) may be either independent for each $i = 1, \dots, n$, in which case the θ_i coefficients are independent *a posteriori*, or they may contain hyperpriors on shared hyperparameters, in which case, θ_i 's are *a posteriori* dependent. We refer to priors of the form (3) as scale-mixture shrinkage priors.

Global-local (GL) shrinkage priors comprise a wide class of scale-mixture shrinkage priors (3). GL priors take the form

$$\theta_i | \tau, \lambda_i \sim N(0, \lambda_i \tau), \quad \lambda_i \sim f, \quad \tau \sim g, \quad (4)$$

where τ is a global shrinkage parameter that shrinks all θ_i 's to the origin, while the local scale parameters λ_i 's control the degree of individual shrinkage. If g puts sufficient mass near zero and f is an appropriately chosen heavy-tailed density, then GL priors in (4) can approximate (2) through a continuous density concentrated near zero with heavy tails. Examples of GL priors include the Bayesian lasso (Park and Casella [24]), the horseshoe prior (Carvalho et al. [10]), the Strawderman-Berger prior (Strawderman [27], Berger [5]), the normal-exponential-gamma (NEG) prior (Griffin and Brown [19]), the generalized double Pareto (GDP) family (Armagan et al. [3]), the horseshoe+ prior (Bhadra et al. [6]), and the three parameter beta normal (TPBN) mixture family (Armagan et al. [2]).

Bhattacharya et al. [7] developed another class of shrinkage priors known as the Dirichlet-kernel (DK) priors. The DK priors replace the single global scale τ in (4) by a vector of scales $(\phi_1 \tau, \dots, \phi_n \tau)$, where $\phi = (\phi_1, \dots, \phi_n)$ is assigned a Dirichlet(a, \dots, a) prior, i.e.

$$\theta_i | \phi_i, \tau \sim \mathcal{K}(\cdot, \phi_i \tau), \quad \phi \sim \text{Dirichlet}(a, \dots, a), \quad \tau \sim g. \quad (5)$$

In (5), \mathcal{K} is any normal scale-mixture density with exponential or heavier tails, such as the Laplace distribution.

GL priors and DK priors have both been studied extensively in the context of sparse normal means estimation. van der Pas et al. [32] showed that by either treating τ in (4) as a tuning parameter that decays to zero at an appropriate rate as $n \rightarrow \infty$ or by giving an empirical Bayes estimate $\hat{\tau}$ based

on an estimate of the sparsity level, the posterior distribution for the horseshoe prior contracts at the (near) minimax rate. Ghosh and Chakrabarti [17] extended the work of van der Pas et al. [32] by showing that when $\tau \rightarrow 0$ at an appropriate rate and the true sparsity level is known, the posterior distribution under a wider class of GL priors (including the student-t prior, the TPBN family, and the GDP family) contracts at the minimax rate. van der Pas et al. [30] gave general sufficient conditions for which the posterior distribution under scale-mixture shrinkage priors of the form (3) achieve the minimax contraction rate, provided that the θ_i 's are *a posteriori* independent.

All the aforementioned results have required the use of tuning parameters or their empirical Bayes estimators. Posterior contraction results for *fully* Bayesian scale-mixture shrinkage priors of the form (3) have been rather sparse in the literature. Bhattacharya et al. [7] were the first ones to show that a fully Bayesian shrinkage prior, belonging to the class of DK priors (5), could achieve minimax posterior contraction. By specifying \mathcal{K} to be the Laplace density and placing an appropriate Gamma prior on τ and an appropriate rate of decay on a in (5), they showed that a variant of the DK prior called the Dirichlet-Laplace prior could achieve the minimax posterior contraction rate. Since then, there do not appear to have been many minimax posterior contraction results for fully Bayesian scale-mixture shrinkage priors. Recently, van der Pas et al. [31] gave sufficient conditions under which the marginal credible sets for a fully Bayesian variant of the horseshoe prior contract at the minimax rate. van der Pas et al. [31] demonstrate that, given an appropriate hyperprior on τ , the horseshoe's $1 - \alpha$ credible intervals and credible balls, $\alpha \in (0, 1)$, have good frequentist coverage. However, their result does not concern contraction of the *entire* posterior distribution. Our paper addresses this theoretical gap by introducing another fully Bayesian scale-mixture shrinkage prior whose posterior density is able to attain the (near) minimax contraction rate. Moreover, the conditions needed to attain the minimax rate of posterior contraction under our prior are much milder than those of Bhattacharya et al. [7].

In addition to robust estimation of $\boldsymbol{\theta}$, we are often interested in identifying the true signals (or non-zero entries) within $\boldsymbol{\theta}$. Here, we are essentially conducting n simultaneous hypothesis tests, H_{0i} : $\theta_i = 0$ vs. H_{1i} : $\theta_i \neq 0, i = 1, \dots, n$. Using the two-components model in (2) as a benchmark, Bogdan et al. [8] studied the risk properties of multiple testing rules within the decision theoretic framework where each θ_i is *truly* generated from a two-groups model. Specifically, Bogdan et al. [8] considered a symmetric 0-1 loss function taken to be the expected total number of misclassified tests.

By imposing a few regularity conditions to induce sparsity and to ensure that the Type I and Type II error probabilities are bounded away from zero and one, Bogdan et al. [8] arrived at a simple closed form for the asymptotic minimum of this loss function. They termed this risk function as the asymptotically Bayes optimal risk under sparsity (or ABOS risk). They then provided necessary and sufficient conditions for which a number of classical multiple test procedures (e.g. the Benjamini and Hochberg [4] procedure) could asymptotically match the ABOS risk, provided that the true θ_i 's come from a two-groups model. A thorough discussion of this decision theoretic framework is presented in Section 5.1.

Testing rules induced by scale-mixture shrinkage priors – specifically GL priors (4) – have also been studied in this decision theoretic framework. Assuming that the θ_i 's come from a two-components model, Datta and Ghosh [12] showed that a thresholding rule based on the posterior mean under the horseshoe prior could asymptotically attain the ABOS risk up to a multiplicative constant. Ghosh et al. [18] generalized this result to a general class of shrinkage priors of the form (4), including the student-t distribution, the TPBN family, and the GDP family of priors. Ghosh and Chakrabarti [17] later showed that their thresholding rule for this same class of priors could even asymptotically attain the ABOS risk exactly. Bhadra et al. [6] also extended this same rule for the horseshoe+ prior. The horseshoe+ prior adds an extra half-Cauchy hyperprior to the hierarchy of the horseshoe prior in order to induce ultra-sparse estimates of $\boldsymbol{\theta}$. Bhadra et al. [6] showed that the horseshoe+ prior could asymptotically attain the ABOS risk up to a multiplicative constant.

In all of these past papers on multiple testing with scale-mixture priors, the global parameter τ in (4) was treated as either a tuning parameter that decays to zero as $n \rightarrow \infty$ or set as a plug-in empirical Bayes estimate $\hat{\tau}$ from van der Pas et al. [32]. To our knowledge, no previous authors have shown that a multiple testing rule induced by a *fully* Bayesian continuous scale-mixture shrinkage prior is able to asymptotically attain the ABOS risk *exactly*. Our work settles this open problem with the introduction of a new scale-mixture shrinkage prior that induces a risk-optimal testing rule.

In this article, we work within the Bayesian framework of priors of the form (3) to address the sparse means problem. Our goal is twofold. Having observed a vector $\mathbf{X} = (X_1, \dots, X_n)$ with entries from (1), we would like to achieve: 1) robust estimation of $\boldsymbol{\theta}$, and 2) a robust testing rule for identifying true signals. To tackle both these problems, we introduce a new scale-mixture shrinkage prior known as the Inverse Gamma-Gamma (IGG) prior. The IGG prior is fully Bayesian and takes a particularly simple form, so it

is completely free of tuning parameters and easy to implement, while still providing strong theoretical guarantees.

The organization of this paper is as follows. In Section 2, we introduce the IGG prior and show that it mimics traditional shrinkage priors by placing heavy mass around zero. In Section 3, we establish various concentration properties of the IGG prior that characterize its tail behavior and that are crucial for establishing our theoretical results. In Section 4, we show that for a class of sparse normal mean vectors, the posterior distribution under the IGG prior contracts around the true θ at (near) minimax rate under mild conditions. In Section 5, we introduce our thresholding rule based on the posterior mean and demonstrate that it asymptotically attains the ABOS risk exactly. In Section 6, we present simulation results which demonstrate that the IGG prior has excellent performance for both estimation and classification in finite samples.

1.4 Notation

We use the following notation for the rest of the paper. Let $\{a_n\}$ and $\{b_n\}$ be two non-negative sequences of real numbers indexed by n , where $b_n \neq 0$ for sufficiently large n . We write $a_n \asymp b_n$ to denote $0 < \liminf_{n \rightarrow \infty} \frac{a_n}{b_n} \leq \limsup_{n \rightarrow \infty} \frac{a_n}{b_n} < \infty$, and $a_n \lesssim b_n$ to denote that there exists a constant $C > 0$ independent of n such that $a_n \leq Cb_n$ provided n is sufficiently large. If $\lim_{n \rightarrow \infty} \frac{a_n}{b_n} = 1$, we write it as $a_n \sim b_n$. Moreover, if $\left| \frac{a_n}{b_n} \right| \leq M$ for all sufficiently large n where $M > 0$ is a positive constant independent of n , then we write $a_n = O(b_n)$. If $\lim_{n \rightarrow \infty} \frac{a_n}{b_n} = 0$, we write $a_n = o(b_n)$. Thus, $a_n = o(1)$ if $\lim_{n \rightarrow \infty} a_n = 0$.

Throughout the paper, we also use Z to denote a standard normal $N(0, 1)$ random variable having cumulative distribution function and probability density function $\Phi(\cdot)$ and $\phi(\cdot)$, respectively.

2 The Inverse Gamma-Gamma (IGG) Prior

Suppose we have observed $\mathbf{X} \sim N(\boldsymbol{\theta}, \mathbf{I}_n)$, and our task is to estimate the n -dimensional vector, $\boldsymbol{\theta}$. Consider putting a scale-mixture prior on each

$\theta_i, i = 1, \dots, n$ of the form

$$\begin{aligned}\theta_i | \lambda_i, \tau_i &\stackrel{\text{ind}}{\sim} N(0, \lambda_i \tau_i), i = 1, \dots, n, \\ \lambda_i &\stackrel{i.i.d.}{\sim} \pi(\lambda_i), i = 1, \dots, n, \\ \tau_i &\stackrel{i.i.d.}{\sim} \tilde{\pi}(\tau_i), i = 1, \dots, n.\end{aligned}\tag{6}$$

The formulation in (6) is similar to the GL priors (4), but not quite the same, since there is not a shared global tuning parameter for all the individual observations. However, one can easily show that the posterior conditional mean is given by

$$\mathbb{E}(\theta_i | X_i, \lambda_i, \tau_i) = \{1 - \kappa_i\} X_i, \tag{7}$$

where $\kappa_i = \frac{1}{1 + \lambda_i \tau_i}$. From (7), it is clear that the amount of shrinkage is controlled by the shrinkage factor κ_i , which depends on both λ_i and τ_i . With appropriately chosen $\pi(\lambda_i)$ and $\tilde{\pi}(\tau_i)$, one can obtain sparse estimates of the θ_i 's.

Consider the following prior, which we call the inverse gamma-gamma prior. For notation, we denote this prior as $\text{IGG}(\lambda, \tau)$.

$$\begin{aligned}\theta_i | \lambda_i, \tau_i &\stackrel{\text{ind}}{\sim} N(0, \lambda_i \tau_i), i = 1, \dots, n, \\ \lambda_i &\stackrel{i.i.d.}{\sim} \text{Inverse Gamma}(a, c), i = 1, \dots, n, \\ \tau_i &\stackrel{i.i.d.}{\sim} \text{Gamma}(b, c), i = 1, \dots, n,\end{aligned}\tag{8}$$

where $a, b, c > 0$. For large values of a , the $\text{Inverse Gamma}(a, c)$ distribution places much more mass around zero, while for very small positive values of b , the $\text{Gamma}(b, c)$ distribution puts much more mass around zero. This gives us some important intuition into the behavior of the IGG prior. As Proposition 1 shows, for any $0 < b < \frac{1}{2}$, the marginal distribution of θ under the IGG prior has a singularity at zero.

Proposition 1. *If $\theta | \lambda, \tau \sim \text{IGG}(\lambda, \tau)$, as in (8), then the marginal distribution of θ is unbounded with a singularity at zero for any $0 < b < 1/2$.*

Proof. See Appendix A. □

Proposition 1 gives us some insight into how we should choose the hyperparameters in (8). Namely, we see that for small values of b , the IGG prior can induce sparse estimates of the θ_i 's by shrinking most observations to zero. As we will illustrate in Section 3, the tails of the IGG prior are still heavy enough to identify signals that are significantly far away from zero.

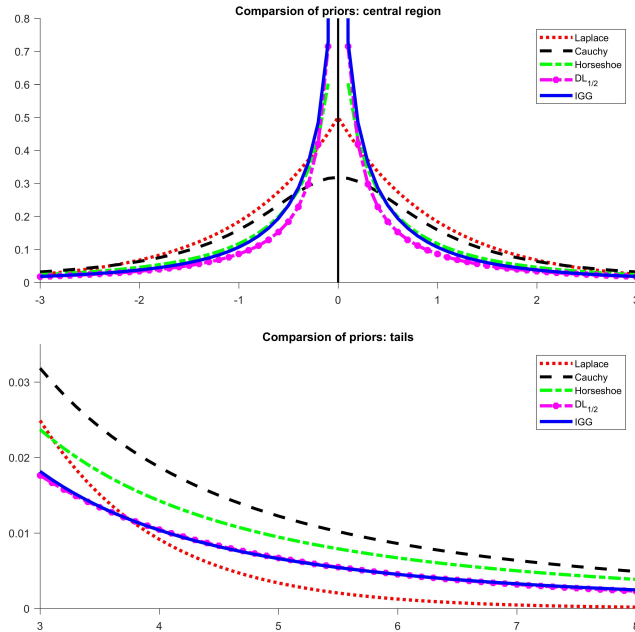


Figure 1: Marginal density of the IGG prior (8) with hyperparameters $a = 0.6, b = 0.4, c = 1$, in comparison to other shrinkage priors. The $DL_{1/2}$ prior is the marginal density for model (5) with a Laplace kernel density and hyperparameter $a = 1/2$.

Figure 1 gives a plot of the marginal density $\pi(\theta_i)$ for the IGG prior (8), with $a = 0.6, b = 0.4$, and $c = 1$. Figure 1 shows that with a small value for b , the IGG has a singularity at zero. The IGG prior also appears to have slightly heavier mass around zero than other well-known scale-mixture shrinkage priors, but the same tail robustness.

3 Concentration Properties of the IGG Prior

Consider the IGG prior given in (8), but now we allow the hyperparameter b_n is allowed to vary with n as $n \rightarrow \infty$. Namely, we allow $0 < b_n < 1$ for all n , but $b_n \rightarrow 0$ as $n \rightarrow \infty$ so that even more mass is placed around zero as $n \rightarrow \infty$. We also fix a to lie in the interval $(\frac{1}{2}, \infty)$. To emphasize that the

hyperparameter b_n depends on n , we rewrite the prior (8) as

$$\begin{aligned}\theta_i | \lambda_i, \tau_i &\stackrel{\text{ind}}{\sim} N(0, \lambda_i \tau_i), i = 1, \dots, n, \\ \lambda_i &\stackrel{i.i.d.}{\sim} \text{Inverse Gamma}(a, c), i = 1, \dots, n, \\ \tau_i &\stackrel{i.i.d.}{\sim} \text{Gamma}(b_n, c), i = 1, \dots, n,\end{aligned}\tag{9}$$

where $b_n \in (0, 1) = o(1)$, $a \in (\frac{1}{2}, \infty)$, $c > 0$. For the rest of the paper, we label this particular variant of the IGG prior as the IGG_n prior.

As described in Section 2, the shrinkage factor $\kappa_i = \frac{1}{1 + \lambda_i \tau_i}$ plays a critical role in the amount of shrinkage of each observation X_i . By (7), we have that the posterior mean under IGG_n prior (9) is given by

$$\mathbb{E}(\theta_i | X_i) = \{\mathbb{E}(1 - \kappa_i) | X_i\} X_i.\tag{10}$$

In this section, we characterize the tail properties of the posterior distribution $\pi(\kappa_i | X_i)$, which demonstrates that the specific IGG_n prior (9) shrinks most estimates of θ_i 's to zero but still has heavy enough tails to identify true signals.

Theorem 1. *Suppose that we observe $X_i \stackrel{\text{ind}}{\sim} N(\theta_i, 1)$, $i = 1, \dots, n$, and that we place the IGG_n prior (9) on each of the θ_i 's. Let $\kappa_i = \frac{1}{1 + \lambda_i \tau_i}$. Then the posterior distribution, $\pi(\kappa_i | X_i)$ is proportional to*

$$\exp\left(-\frac{\kappa_i X_i^2}{2}\right) \kappa_i^{a-1/2} (1 - \kappa_i)^{b_n-1}, \quad \kappa_i \in (0, 1).\tag{11}$$

Proof. See Appendix A. □

Using Theorem 1, we now prove three concentration properties of κ_i and give four corresponding corollaries. Again, we assume the IGG_n prior on θ_i for $X_i \sim N(\theta_i, 1)$ for all of these results.

Theorem 2. *For any $a, b_n \in (0, \infty)$,*

$$\mathbb{E}(1 - \kappa_i | X_i) \leq e^{X_i^2/2} \left(\frac{b_n}{a + b_n + 1/2} \right).$$

Proof. See Appendix A. □

Corollary 2.1. *If a is fixed and $b_n \rightarrow 0$ as $n \rightarrow \infty$, then $\mathbb{E}(1 - \kappa_i | X_i) \rightarrow 0$ as $n \rightarrow \infty$.*

Theorem 3. Fix $\epsilon \in (0, 1)$. For any $a \in (\frac{1}{2}, \infty)$, $b_n \in (0, 1)$,

$$P(\kappa_i < \epsilon | X_i) \leq e^{X_i^2/2} \frac{b_n \epsilon}{(a + 1/2)(1 - \epsilon)}.$$

Proof. See Appendix A. □

Corollary 3.1. If $a \in (\frac{1}{2}, \infty)$ is fixed and $b_n \rightarrow 0$ as $n \rightarrow \infty$, then by Theorem 3, $P(\kappa_i \geq \epsilon | X_i) \rightarrow 1$ for any fixed $\epsilon \in (0, 1)$.

Theorem 4. Fix $\eta \in (0, 1)$, $\delta \in (0, 1)$. Then for any $a \in (\frac{1}{2}, \infty)$ and $b_n \in (0, 1)$,

$$P(\kappa_i > \eta | X_i) \leq \frac{(a + \frac{1}{2})(1 - \eta)^{b_n}}{b_n(\eta\delta)^{a+\frac{1}{2}}} \exp\left(-\frac{\eta(1 - \delta)}{2} X_i^2\right).$$

Proof. See Appendix A. □

Corollary 4.1. For any fixed n where $a \in (\frac{1}{2}, \infty)$, $b_n \in (0, 1)$, and for every fixed $\eta \in (0, 1)$, $P(\kappa_i \leq \eta | X_i) \rightarrow 1$ as $X_i \rightarrow \infty$.

Corollary 4.2. For any fixed n where $a \in (\frac{1}{2}, \infty)$, $b_n \in (0, 1)$, and for every fixed $\eta \in (0, 1)$, $E(1 - \kappa_i | X_i) \rightarrow 1$ as $X_i \rightarrow \infty$.

Since $\mathbb{E}(\theta_i | X_i) = \{\mathbb{E}(1 - \kappa_i) | X_i\} X_i$, Corollaries 2.1 and 3.1 illustrate that all observations will be shrunk towards the origin under the IGG_n prior (9). However, Corollaries 4.1 and 4.2 demonstrate that if X_i is big enough, then the posterior mean $\{\mathbb{E}(1 - \kappa_i) | X_i\} X_i \approx X_i$. This assures us that the tails of the IGG prior are still sufficiently heavy to detect true signals.

We will use the concentration properties established in Theorem 2 and 4 to provide sufficient conditions for which the posterior mean and posterior distribution under the IGG_n prior (9) contract around the true θ_0 at minimax or near-minimax rate in Section 4. These concentration properties will also help us to construct the multiple testing procedure based on κ_i in Section 5.

4 Posterior Contraction of the IGG Prior

4.1 Sparse Normal Vectors in the Nearly Black Sense

Suppose that we observe $\mathbf{X} = (X_1, \dots, X_n) \in \mathbb{R}^n$ from (1). Let $\ell_0[q_n]$ denote the subset of \mathbb{R}^n given by

$$\ell_0[q_n] = \{\boldsymbol{\theta} \in \mathbb{R}^n : \#(1 \leq j \leq n : \theta_j \neq 0) \leq q_n\}. \quad (12)$$

If $\boldsymbol{\theta} \in \ell_0[q_n]$ with $q_n = o(n)$ as $n \rightarrow \infty$, we say that $\boldsymbol{\theta}$ is sparse in the “nearly black sense.” Let $\boldsymbol{\theta}_0 = (\theta_{01}, \dots, \theta_{0n})$ be the true mean vector. In their seminal work, Donoho et al. [13] showed that for any estimator of $\boldsymbol{\theta}$, denoted by $\hat{\boldsymbol{\theta}}$, the corresponding minimax risk with respect to the l_2 - norm is given by

$$\inf_{\hat{\boldsymbol{\theta}}} \sup_{\boldsymbol{\theta}_0 \in \ell_0[q_n]} \mathbb{E}_{\boldsymbol{\theta}_0} \|\hat{\boldsymbol{\theta}} - \boldsymbol{\theta}_0\|^2 = 2q_n \log\left(\frac{n}{q_n}\right) (1 + o(1)), \text{ as } n \rightarrow \infty. \quad (13)$$

In (13) and throughout the paper, $\mathbb{E}_{\boldsymbol{\theta}_0}$ denotes expectation with respect to the $N_n(\boldsymbol{\theta}_0, \mathbf{I}_n)$ distribution. (13) effectively states that in the presence of sparsity, a minimax-optimal estimator only loses as a logarithmic factor (in the ambient dimension) as a penalty for not knowing the true locations of the zeroes. Moreover, (13) implies that we only need a number of replicates in the order of the true sparsity level q_n to consistently estimate $\boldsymbol{\theta}_0$. In order for the performance of Bayesian estimators to be compared with frequentist ones, we say that a Bayesian point estimator $\hat{\boldsymbol{\theta}}^B$ attains the minimax risk (in the order of a constant) if

$$\sup_{\boldsymbol{\theta}_0 \in \ell_0[q_n]} \mathbb{E}_{\boldsymbol{\theta}_0} \|\hat{\boldsymbol{\theta}}^B - \boldsymbol{\theta}_0\|^2 \asymp q_n \log\left(\frac{n}{q_n}\right). \quad (14)$$

Examples of potential choices for $\hat{\boldsymbol{\theta}}^B$ include the posterior median or the posterior mean (as in Johnstone and Silverman [21]), or the posterior mode (as in Ročková [25]). (14) pertains only to a particular point estimate. For a *fully* Bayesian interpretation, we say that the posterior distribution contracts around the true $\boldsymbol{\theta}_0$ at a rate at least as fast as the minimax l_2 risk if

$$\sup_{\boldsymbol{\theta}_0 \in \ell_0[q_n]} \mathbb{E}_{\boldsymbol{\theta}_0} \Pi\left(\boldsymbol{\theta} : \|\boldsymbol{\theta} - \boldsymbol{\theta}_0\|^2 > M_n q_n \log\left(\frac{n}{q_n}\right) \mid \mathbf{X}\right) \rightarrow 0, \quad (15)$$

for every $M_n \rightarrow \infty$ as $n \rightarrow \infty$. On the other hand, in another seminal paper, Ghosal et al. [16] showed that the posterior distribution cannot contract faster than the minimax rate of $q_n \log\left(\frac{n}{q_n}\right)$ around the truth. Hence, the optimal rate of contraction of a posterior distribution around the true $\boldsymbol{\theta}_0$ must be the minimax optimal rate in (13), up to some multiplicative constant. In other words, if we use a fully Bayesian model to estimate a “nearly black” normal mean vector, the minimax optimal rate should be our benchmark, and the posterior distribution should capture the true $\boldsymbol{\theta}_0$ in a ball of squared radius at most $q_n \log\left(\frac{n}{q_n}\right)$ (up to a multiplicative constant) as $n \rightarrow \infty$.

It should be remarked that in practice, many Bayesian point estimators and prior distributions require the true sparsity level q_n to be known in order

to attain the minimax rate of contraction. This information is rarely available, so the best we can do in most instances is attain posterior contraction at the *near*-minimax rate of $q_n \log n$.

In the subsequent section, we provide sufficient conditions on the rate of decay of b_n in (9) such that, under the IGG_n prior, the posterior mean attains the minimax risk, while the posterior distribution contracts at the minimax rate. In order for (14) and (15) to hold for the IGG_n prior, the true sparsity level q_n must be known. However, if q_n is unknown, then the IGG_n prior can still attain near-minimax concentration rates.

4.2 Optimal Posterior Contraction Under the IGG Prior

In this section, we study the mean square error (MSE) and the posterior variance of the IGG prior and provide an upper bound on both. For all our results, we assume that the true θ_0 belongs to the set of nearly black vectors defined by (12). With a suitably chosen rate for b_n in (9), these upper bounds are equal, up to a multiplicative constant, to the minimax risk. Utilizing these bounds, we also show that the posterior distribution under the IGG_n prior (9) is able to contract around θ_0 at minimax-optimal rates.

Since the priors (9) are independently placed on each $\theta_i, i = 1, \dots, n$, we have that $\mathbb{E}(\theta|X_i) = (1 - \mathbb{E}(\kappa_i|X_i))X_i$ for $i = 1, \dots, n$. Thus, we denote the resulting vector of posterior means $(\mathbb{E}(\theta_1|X_1), \dots, \mathbb{E}(\theta_n|X_n))$ by $T(\mathbf{X})$ and the i th individual posterior mean by $T(X_i)$. Therefore, $T(\mathbf{X})$ is the Bayes estimate of θ under squared error loss. Theorem 5 gives an upper bound on the mean squared error for $T(\mathbf{X})$.

Theorem 5. *Suppose $\mathbf{X} \sim N_n(\theta_0, \mathbf{I}_n)$, where $\theta_0 \in \ell_0[q_n]$. Let $T(\mathbf{X})$ denote the posterior mean vector under (9). If $a \in (\frac{1}{2}, \infty)$, $b_n \in (0, 1)$ with $b_n \rightarrow 0$ as $n \rightarrow \infty$, the MSE satisfies*

$$\sup_{\theta_0 \in \ell_0[q_n]} \mathbb{E}_{\theta_0} \|T(\mathbf{X}) - \theta_0\|^2 \lesssim q_n \log \left(\frac{1}{b_n} \right) + (n - q_n) b_n \sqrt{\log \left(\frac{1}{b_n} \right)},$$

provided that $q_n \rightarrow \infty$ and $q_n = o(n)$ as $n \rightarrow \infty$.

Proof. See Appendix B. □

By the minimax result in Donoho et al. [13], we also have the lower bound,

$$\sup_{\theta_0 \in \ell_0[q_n]} \mathbb{E}_{\theta_0} \|T(\mathbf{X}) - \theta_0\|^2 \geq 2q_n \log \left(\frac{n}{q_n} \right) (1 + o(1)),$$

as $n, q_n \rightarrow \infty$ and $q_n = o(n)$. The choice of $b_n = \left(\frac{q_n}{n}\right)^\alpha$, for $\alpha \geq 1$, therefore leads to an upper bound MSE of order $q_n \log\left(\frac{n}{q_n}\right)$ with a multiplicative constant of at most 2α . Based on these observations, we immediately have the following corollary.

Corollary 5.1. *Suppose that q_n is known, and that we set $b_n = \left(\frac{q_n}{n}\right)^\alpha$, where $\alpha \geq 1$. Then under the conditions of Theorem 5,*

$$\sup_{\boldsymbol{\theta}_0 \in \ell_0[q_n]} \mathbb{E}_{\boldsymbol{\theta}_0} \|\mathbf{T}(\mathbf{X}) - \boldsymbol{\theta}_0\|^2 \asymp q_n \log\left(\frac{n}{q_n}\right).$$

Corollary 5.1 shows that the posterior mean under the IGG prior performs well as a point estimator for $\boldsymbol{\theta}_0$, as it is able to attain the minimax risk (possibly up to a multiplicative constant of at most 2 for $\alpha = 1$). Although the IGG prior does not include a point mass at zero, Proposition 1 and Corollary 5.1 together show that the pole at zero for the IGG prior mimics the point mass well enough, while the heavy tails ensure that large observations are not over-shrunk.

The next theorem gives an upper bound for the total posterior variance corresponding to the IGG $_n$ (9) prior.

Theorem 6. *Suppose $\mathbf{X} \sim N_n(\boldsymbol{\theta}_0, \mathbf{I}_n)$, where $\boldsymbol{\theta}_0 \in \ell_0[q_n]$. Under prior (7) and the conditions of Theorem 5, the total posterior variance satisfies*

$$\sup_{\boldsymbol{\theta}_0 \in \ell_0[q_n]} \mathbb{E}_{\boldsymbol{\theta}_0} \sum_{i=1}^n \text{Var}(\theta_{0i} | X_i) \lesssim q_n \log\left(\frac{1}{b_n}\right) + (n - q_n) b_n \sqrt{\log\left(\frac{1}{b_n}\right)},$$

provided that $q_n \rightarrow \infty$ and $q_n = o(n)$ as $n \rightarrow \infty$.

Proof. See Appendix B. □

Having proven Theorems 5 and 6, we are now ready to state our main theorem concerning optimal posterior contraction. Theorem 7 shows that the IGG is competitive with other popular heavy-tailed priors like the global-local shrinkage priors considered in Ghosh and Chakrabarti [17] or the Dirichlet-Laplace prior considered by Bhattacharya et al. [7]. As before, we denote the posterior mean vector under (9) as $\mathbf{T}(\mathbf{X})$.

Theorem 7. *Suppose $\mathbf{X} \sim N_n(\boldsymbol{\theta}_0, \mathbf{I}_n)$, where $\boldsymbol{\theta}_0 \in \ell_0[q_n]$. Suppose that the true sparsity level q_n is known, with $q_n \rightarrow \infty$, and $q_n = o(n)$ as $n \rightarrow \infty$. Under prior (9), with $a \in (\frac{1}{2}, \infty)$ and $b_n = \left(\frac{q_n}{n}\right)^\alpha$, $\alpha \geq 1$,*

$$\sup_{\boldsymbol{\theta}_0 \in \ell_0[q_n]} \mathbb{E}_{\boldsymbol{\theta}_0} \Pi\left(\boldsymbol{\theta} : \|\boldsymbol{\theta} - \boldsymbol{\theta}_0\|^2 > M_n q_n \log\left(\frac{n}{q_n}\right) \mid \mathbf{X}\right) \rightarrow 0, \quad (16)$$

and

$$\sup_{\boldsymbol{\theta}_0 \in \ell_0[q_n]} \mathbb{E}_{\boldsymbol{\theta}_0} \Pi \left(\boldsymbol{\theta} : \|\boldsymbol{\theta} - T(\mathbf{X})\|^2 > M_n q_n \log \left(\frac{n}{q_n} \right) \middle| \mathbf{X} \right) \rightarrow 0, \quad (17)$$

for every $M_n \rightarrow \infty$ as $n \rightarrow \infty$.

Proof. A straightforward application of Markov's inequality combined with the results of Theorems 5 and 6 leads to (16), while (17) follows from Markov's inequality combined with only the result of Theorem 6. \square

Theorem 7 shows that under mild regularity conditions, the posterior distribution under the IGG prior contracts around both the true mean vector *and* the corresponding Bayes estimates at least as fast as the minimax l_2 risk in (13). Since the posterior distribution cannot contract around the truth faster than the rate of $q_n \log \left(\frac{n}{q_n} \right)$ (by Ghosal et al. [16]), the posterior distribution for the IGG prior under the conditions of Theorem 7 must contract around the true $\boldsymbol{\theta}_0$ at the minimax optimal rate in (13) up to some multiplicative constant.

To our knowledge, our result for the IGG prior is only the second time that the posterior distribution for a *fully* Bayesian scale-mixture shrinkage prior (3) has been shown to contract around the true nearly black vector at minimax rate. Previously, Bhattacharya et al. [7] showed that the Dirichlet-Laplace prior, a specific variant of (5), contracts around $\boldsymbol{\theta}_0$ at the minimax rate, provided that $\|\boldsymbol{\theta}_0\|_2^2 \leq q_n \log^4 n$ if $a = n^{-(1+\beta)}$, or provided that $q_n \gtrsim \log n$ if $a = \frac{1}{n}$. The IGG_n prior (9) removes these restrictions on $\boldsymbol{\theta}_0$ and q_n . The IGG prior does not require $\boldsymbol{\theta}_0$ to lie in a ball of a certain squared radius nor does it place any restrictions on the sparsity level q_n (other than the standard assumptions $q_n \rightarrow \infty$ as $n \rightarrow \infty$ and $q_n = o(n)$) in order to attain the minimax rate for posterior contraction.

In reality, the true sparsity level of q_n is rarely known, so the best that we can do is to obtain the near-minimax contraction rate of $q_n \log n$. A suitable modification of Theorem 7 leads to the following corollary.

Corollary 7.1. *Suppose $\mathbf{X} \sim N_n(\boldsymbol{\theta}_0, \mathbf{I}_n)$, where $\boldsymbol{\theta}_0 \in \ell_0[q_n]$. Suppose that the true sparsity level q_n is unknown, but that $q_n \rightarrow \infty$, and $q_n = o(n)$ as $n \rightarrow \infty$. Under prior (9), with $a \in (\frac{1}{2}, \infty)$ and $b_n = \frac{1}{n^\alpha}$, $\alpha \geq 1$, then*

$$\sup_{\boldsymbol{\theta}_0 \in \ell_0[q_n]} \mathbb{E}_{\boldsymbol{\theta}_0} \Pi \left(\boldsymbol{\theta} : \|\boldsymbol{\theta} - \boldsymbol{\theta}_0\|^2 > M_n q_n \log n \middle| \mathbf{X} \right) \rightarrow 0, \quad (18)$$

and

$$\sup_{\boldsymbol{\theta}_0 \in \ell_0[q_n]} \mathbb{E}_{\boldsymbol{\theta}_0} \Pi \left(\boldsymbol{\theta} : \|\boldsymbol{\theta} - T(\mathbf{X})\|^2 > M_n q_n \log n \middle| \mathbf{X} \right) \rightarrow 0, \quad (19)$$

for every $M_n \rightarrow \infty$ as $n \rightarrow \infty$.

Having shown that the posterior mean under (9) attains the minimax risk up to a multiplicative constant, and that its posterior density captures the true $\boldsymbol{\theta}_0$ in a ball of squared radius at most $q_n \log n$ up to some multiplicative constant, we now demonstrate how the IGG prior can be used in the context of multiple hypothesis testing to identify true signals.

5 Multiple Testing with the IGG Prior

5.1 Asymptotic Bayes Optimality Under Sparsity

Suppose we observe $\mathbf{X} = (X_1, \dots, X_n)$, such that $X_i \sim N(\theta_i, 1)$, for $i = 1, \dots, n$. To identify the true signals in \mathbf{X} , we conduct n simultaneous tests: $H_{0i} : \theta_i = 0$ against $H_{1i} : \theta_i \neq 0$, for $i = 1, \dots, n$. For each i , θ_i is assumed to be a random variable whose distribution is determined by the latent binary random variable ν_i , where $\nu_i = 0$ denotes the event that H_{0i} is true, while $\nu_i = 1$ corresponds to the event that H_{0i} is false. Here ν_i 's are assumed to be i.i.d. Bernoulli(p) random variables, for some p in $(0, 1)$. Under H_{0i} , i.e. $\theta_i \sim \delta_{\{0\}}$, the distribution having a mass 1 at 0, while under H_{1i} , $\theta_i \neq 0$ and is assumed to follow an $N(0, \psi^2)$ distribution with $\psi^2 > 0$. Thus.

$$\theta_i \stackrel{i.i.d.}{\sim} (1-p)\delta_{\{0\}} + pN(0, \psi^2), i = 1, \dots, n. \quad (20)$$

The marginal distributions of the X_i 's are then given by the following two-groups model:

$$X_i \stackrel{i.i.d.}{\sim} (1-p)N(0, 1) + pN(0, 1 + \psi^2), i = 1, \dots, n. \quad (21)$$

Our testing problem is now equivalent to testing simultaneously

$$H_{0i} : \nu_i = 0 \text{ versus } H_{1i} : \nu_i = 1 \text{ for } i = 1, \dots, n. \quad (22)$$

We consider a symmetric 0-1 loss for each individual test and the total loss of a multiple testing procedure is assumed to be the sum of the individual losses incurred in each test. Letting t_{1i} and t_{2i} denote the probabilities of type I and type II errors of the i th test respectively, the Bayes risk of a multiple testing procedure under the two-groups model (1) is given by

$$R = \sum_{i=1}^m \{(1-p)t_{1i} + pt_{2i}\}. \quad (23)$$

Bogdan et al. [8] showed that the rule which minimizes the Bayes risk in (23) is the test which, for each $i = 1, \dots, n$, rejects H_{0i} if

$$\frac{f(x_i|\nu_i = 1)}{f(x_i|\nu_i = 0)} > \frac{1-p}{p}, \text{ i.e. } X_i^2 > c^2, \quad (24)$$

where $f(x_i|\nu_i = 1)$ denotes the marginal density of X_i under H_{1i} , while $f(x_i|\nu_i = 0)$ denotes that under H_{0i} and $c^2 \equiv c_{\psi, f}^2 = \frac{1+\psi^2}{\psi^2}(\log(1+\psi^2) + 2\log(f))$, with $f = \frac{1-p}{p}$. The above rule is known as the Bayes Oracle, because it makes use of unknown parameters ψ and p , and hence, it is not attainable in finite samples. By reparametrizing as $u = \psi^2$ and $v = uf^2$, the above threshold becomes

$$c^2 \equiv c_{u,v}^2 = \left(1 + \frac{1}{u}\right) \left(\log v + \log\left(1 + \frac{1}{u}\right)\right).$$

Bogdan et al. [8] considered the following asymptotic scheme.

Assumption 1

The sequences of vectors (ψ_n, p_n) satisfies the following conditions:

1. $p_n \rightarrow 0$ as $n \rightarrow \infty$.
2. $u_n = \psi_n^2 \rightarrow \infty$ as $n \rightarrow \infty$.
3. $v_n = u_n f^2 = \psi_n^2 \left(\frac{1-p_n}{p_n}\right)^2 \rightarrow \infty$ as $n \rightarrow \infty$.
4. $\frac{\log v_n}{u_n} \rightarrow C \in (0, \infty)$ as $n \rightarrow \infty$.

Bogdan et al. [8] provided detailed insight on the threshold C . Summarizing briefly, if $C = 0$, then both the Type I and Type II errors are zero, and for $C = \infty$, the inference is essentially no better than tossing a coin. Under Assumption 1, Bogdan et al. [8] showed that the corresponding asymptotic optimal Bayes risk has a particularly simple form, which is given by

$$R_{Opt}^{BO} = n((1-p)t_1^{BO} + pt_2^{BO}) = np(2\Phi(\sqrt{C}) - 1)(1 + o(1)), \quad (25)$$

where the $o(1)$ terms tend to zero as $n \rightarrow \infty$. A testing procedure with risk R is said to be asymptotically Bayes optimal under sparsity (ABOS) if

$$\frac{R}{R_{Opt}^{BO}} \rightarrow 1 \text{ as } n \rightarrow \infty. \quad (26)$$

5.2 An Optimal Testing Rule Based on the IGG Estimator

As noted earlier, the posterior mean depends heavily on the shrinkage factor, $\kappa_i = \frac{1}{\lambda_i \tau_i + 1}$. Because of the concentration properties of the IGG prior proven in Sections 3 and 4, a sensible thresholding rule classifies observations as signals or as noise based on the posterior distribution of this shrinkage factor. Consider the following testing rule for the i th observation X_i :

$$\text{Reject } H_{0i} \text{ if } \mathbb{E}(1 - \kappa_i | X_i) > \frac{1}{2}, \quad (27)$$

where κ_i is the shrinkage factor based on the IGG_n prior (9). We have already seen from Theorem 1 and Theorem 5 that the IGG prior (8) mimics the point-mass mixture model (2) as far as estimation of θ is concerned. Analogously, within the context of multiple testing, a good benchmark for our test procedure (27) should be whether it is ABOS, i.e. whether its optimal risk is asymptotically equal to that of the Bayes Oracle risk. Adopting the framework of Bogdan et al. [8], we let R_{IGG} denote the asymptotic Bayes risk of testing rule (27), and we compare it to the ABOS risk defined in (25).

The next theorem illustrates that in the presence of sparsity, rule (27) is in fact ABOS.

Theorem 8. *Suppose that X_1, \dots, X_n are i.i.d. observations having distribution (21) where the sequence of vectors (ψ^2, p) satisfies Assumption 1. Suppose we wish to test (22) using the classification rule (27). Suppose further that $a \in (\frac{1}{2}, \infty)$ and $b_n \in (0, 1)$, with $b_n \rightarrow 0$ as $n \rightarrow \infty$ in such a way that $\lim_{n \rightarrow \infty} \frac{b_n^{1/4}}{p_n} \in (0, \infty)$. Then*

$$\lim_{n \rightarrow \infty} \frac{R_{IGG}}{R_{Opt}^{BO}} = 1, \quad (28)$$

i.e. rule (27) based on the IGG_n prior (9) is ABOS.

Proof. See Appendix C. □

We have shown that our thresholding rule based on the IGG_n prior asymptotically attains the ABOS risk exactly, provided that b_n decays to zero at a certain rate relative to the sparsity level p . For example, if the prior mixing proportion p_n is known, we can set the hyperparameter $b_n = p_n^4$. Then the conditions for classification rule (27) to be ABOS are satisfied.

Our work appears to be the first result in the literature to illustrate that a thresholding rule based on the posterior mean of a *fully* Bayesian normal

scale-mixture shrinkage prior (3) is ABOS. All previous results on thresholding procedures based on the posterior means of global-local shrinkage priors (4) (such as those in Datta and Ghosh [12], Ghosh et al. [18], Bhadra et al. [6], and Ghosh and Chakrabarti [17]) have required the use of tuning parameters or empirical Bayes plug-in estimators to achieve the ABOS risk asymptotically (possibly up to a multiplicative constant).

In this sense, the IGG prior not only matches the performance of a more natural two-components mixture prior as a classification rule for signals, but it presents an advantage over global-local shrinkage priors. In order to optimally classify signals vs. noise, it does *not* require the estimation of a global tuning parameter, but can instead, rely on a fully Bayesian formulation in order to achieve optimal risk properties. Strictly speaking, the IGG prior does not fall within the class of GL priors, since it does not utilize a shared parameter τ . However, we do not view this as a handicap, so long as the prior has good theoretical properties and allows us to identify true signals with high probability. We have seen that the IGG prior and the associated thresholding rule (27) do just that.

6 Simulations

6.1 Computation and Selection of Hyperparameters

Letting $\kappa_i = \frac{1}{1+\lambda_i\tau_i}$, the full conditional distributions for (8) are

$$\begin{aligned} \theta_i \mid \text{rest} &\sim N((1 - \kappa_i)X_i, 1 - \kappa_i), i = 1, \dots, n, \\ \lambda_i \mid \text{rest} &\sim \text{Inverse Gamma} \left(a + \frac{1}{2}, \frac{\theta_i^2}{2\tau_i} + c \right), i = 1, \dots, n, \\ \tau_i \mid \text{rest} &\sim \text{giG} \left(\frac{\theta_i^2}{\lambda_i}, 2c, b - \frac{1}{2} \right), i = 1, \dots, n, \end{aligned} \quad (29)$$

where $\text{giG}(a, b, p)$ denotes a generalized inverse Gaussian (giG) density with $f(x; a, b, p) \propto x^{(p-1)} e^{-(a/x + bx)/2}$. Therefore, the IGG model (8) can be implemented straightforwardly with Gibbs sampling, utilizing the full conditionals in (29).

For all our simulations, we set $a = c = 1$, so that the Inverse Gamma prior on the λ_i 's is heavily concentrated near zero. However, the choices of a and c are not critical, as long as $a > \frac{1}{2}$. Based on Corollary 7.1, we recommend setting $b = \frac{1}{n}$. This is not only simple to interpret, but it ensures that the IGG posterior distribution will contract around the true θ_0 at least at near-minimax rate up to some multiplicative constant.

n	100						200					
	5		10		20		5		10		20	
A	7	8	7	8	7	8	7	8	7	8	7	8
IGG _{1/n}	8.25	7.58	13.62	12.63	28.24	25.99	14.17	13.11	29.36	27.10	55.40	51.00
BL	41.93	41.96	46.33	46.36	60.04	60.08	78.38	78.43	95.52	95.51	120.97	121.03
HS	9.00	8.64	16.19	15.67	35.08	35.14	18.07	17.83	33.57	32.42	69.86	68.37
DL	8.36	7.44	13.80	12.72	29.12	26.51	14.21	12.90	30.20	27.51	56.98	52.20
PM-EB	8.77	8.51	14.75	14.34	31.01	30.13	14.58	14.44	30.79	29.91	61.23	59.50

Table 1: Comparison of average squared error loss for the posterior median estimate of θ across 100 replications. Results are reported for the IGG_{1/n} (Inverse Gamma-Gamma with $b = 1/n$), BL (Bayesian Lasso), HS (horseshoe), DL (Dirichlet-Laplace), and PM-EB (point mass mixture with empirical Bayes estimate for p and a Cauchy distribution for the slab).

We denote our IGG prior with hyperparameter $b = \frac{1}{n}$ as IGG_{1/n}. For both of the simulation studies described below, we run 10,000 iterations of a Gibbs sampler, discarding the first 5000 as burn-in.

6.2 Simulation Study for Sparse Estimation

To illustrate finite-sample performance of the IGG_{1/n} prior, we use the setup in Bhattacharya et al. [7] where we pre-specify sparsity levels of $q_n/n = 0.05, 0.10$, and 0.20 , and set the signals all equal to values of either $A = 7$ or 8 . We use sample sizes of $n = 100$ and $n = 200$ with different q_n and A , for a total of 12 simulation settings. We compute the average squared error loss corresponding to the posterior median across 100 replicates.

We compare our results for IGG_{1/n} to the average squared error loss of the posterior median under the Bayesian Lasso (BL), the horseshoe (HS), the Dirichlet-Laplace (DL), and the point mass mixture prior (PM-EB) by Johnstone and Silverman [20]. For the HS prior, we use a fully Bayesian approach, with $\tau \sim C^+(0, 1)$, as in Ghosh et al. [18]. For the DL prior, we specify a Laplace kernel density and $a = \frac{1}{n}$ in (5), as in Bhattacharya et al. [7]. For the PM-EB, we use the `EbayesThresh` R package to implement a spike-and-slab density (2) with an empirical Bayes estimate for the mixing proportion p and a Cauchy distribution to model the “slab.” Our results are presented in Table 1.

Table 1 shows that under these various sparsity and signal strength settings, the IGG_{1/n}’s posterior median has the lowest (estimated) squared error loss in nearly all of the simulation settings. It performs better than the horseshoe in all settings, and when compared to the Bayesian Lasso, the

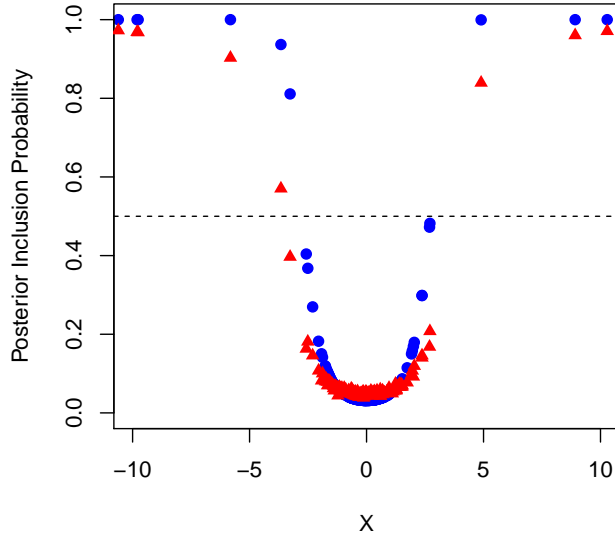


Figure 2: Comparison between the posterior inclusion probabilities and the posterior shrinkage weights $1 - \mathbb{E}(\kappa_i|X_i)$ when $p = 0.10$.

IGG_{1/n} performs significantly better. This is because the BL has insufficiently heavy tails and tends to overshrink the signals, while undershrinking noise. Our empirical results confirm the theoretical properties that were proven in Sections 3 and 4 and illustrate that for finite samples, the IGG prior often outperforms other popular shrinkage priors.

6.3 Simulation Study for Multiple Testing

For the multiple testing rule (27), we adopt the simulation framework of Datta and Ghosh [12] and Ghosh et al. [18] and fix sparsity levels at $p \in \{0.01, 0.05, 0.10, 0.15, 0.2, 0.25, 0.3, 0.35, 0.4, 0.45, 0.5\}$ for a total of 11 simulation settings. For sample size $n = 200$ and each p , we generate data from the two-groups model (20), with $\psi = \sqrt{2 \log n} = 3.26$. We then apply the thresholding rule (27) using IGG_{1/n} to classify θ_i 's in our model as either signals ($\theta_i \neq 0$) or noise ($\theta_i = 0$). We estimate the average misclassification probability (MP) for the thresholding rule (27) from 100 replicates.

Taking $p = 0.10$, we plot in Figure 2 the theoretical posterior inclusion probabilities $\omega_i(X_i) = P(\nu_i = 1|X_i)$ for the two-groups model (20) given by

$$\omega_i(X_i) = \pi(\nu_i = 1|X_i) = \left\{ \left(\frac{1-p}{p} \right) \sqrt{1 + \psi^2} e^{-\frac{X_i^2}{2} \frac{\psi^2}{1+\psi^2}} + 1 \right\}^{-1},$$

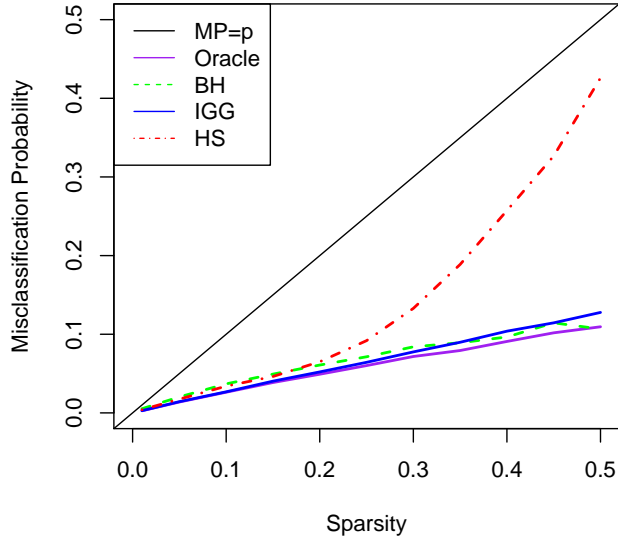


Figure 3: Estimated misclassification probabilities. Thresholding rule (27) based on the IGG posterior mean is nearly as good as the Bayes Oracle (24).

along with the shrinkage weights $1 - \mathbb{E}(\kappa_i|X_i)$ corresponding to the $\text{IGG}_{1/n}$ prior. The circles in the figure denote the theoretical posterior inclusion probabilities, while the triangles correspond to the shrinkage weights $1 - \mathbb{E}(\kappa_i|X_i)$. The figure clearly shows that for small values of the sparsity level p , the shrinkage weights are in close proximity to the posterior inclusion probabilities. This and the theoretical results established in Section 5 justify the use of using $1 - \mathbb{E}(\kappa_i|X_i)$ as an approximation to the corresponding posterior inclusion probabilities $\omega_i(X_i)$ in sparse situations. Therefore, this motivates the use of the $\text{IGG}_{1/n}$ prior (9) and its corresponding decision rule (27) for identifying signals in noisy data.

Figure 3 shows the estimated misclassification probabilities (MP) for decision rule (27) for the $\text{IGG}_{1/n}$ prior, along with the estimated MP's for the Bayes Oracle (BO), the Benjamini-Hochberg procedure (BH), and the horseshoe (HS). The Bayes Oracle rule, defined in (24), is the decision rule that minimizes the expected number of misclassified signals (23) when (p, ψ) are known. The Bayes Oracle therefore serves as the lower bound to the MP, whereas the line $MP = p$ corresponds to the situation where we reject all null hypotheses without looking into the data. For the Benjamini-Hochberg rule, we use $\alpha_n = 1/\log n = 0.1887$. Bogdan et al. [8] theoretically established the ABOS property of the BH procedure for this choice of α_n . For the

horseshoe, we use the classification rule

$$\text{Reject } H_{0i} \text{ if } \mathbb{E}(1 - \kappa_i | X_1, \dots, X_n) > \frac{1}{2}, \quad (30)$$

where $\kappa_i = \frac{1}{1 + \lambda_i^2 \tau^2}$, $\lambda_i \sim C^+(0, 1)$, and $\tau \sim C^+(0, 1)$. Since τ is a shared global parameter, the posterior for κ_i depends on *all* the data. Carvalho et al. [10] first introduced thresholding rule (30) for the horseshoe. Datta and Ghosh [12] studied the theoretical properties of this thresholding rule for the horseshoe, treating τ as a tuning parameter. Ghosh et al. [18] later extended rule (30) for a general class of global-local shrinkage priors (4), which includes the Strawderman-Berger, normal-exponential-gamma, and generalized double Pareto priors. Based on Ghosh et al. [18]’s simulation results, the HS performs similarly as or better than these other aforementioned priors, so we only compare the performance of the $\text{IGG}_{1/n}$ prior with that of the HS.

Our results provide strong support to our theoretical findings in Section 5 and strong justification for the use of (27) to classify signals. As Figure 3 illustrates, the performance for rule (30) under the horseshoe degrades considerably as $\boldsymbol{\theta} = (\theta_1, \dots, \theta_n)$ becomes more dense. With sparsity level $p = 0.5$, the horseshoe’s misclassification rate is close to 0.4, only marginally better than rejecting all the null hypotheses without looking at the data. In contrast, Figure 3 shows that the classification rule (27) under the $\text{IGG}_{1/n}$ prior is robust no matter what the actual sparsity level of $\boldsymbol{\theta}$ is. Even when $p = 0.5$, it performs nearly as well as the Bayes Oracle. These empirical results demonstrate that $\text{IGG}_{1/n}$ is not only excellent for estimating $\boldsymbol{\theta}$ but also for classifying signals.

Finally, we demonstrate the shrinkage properties corresponding to the $\text{IGG}_{1/n}$ prior along with the horseshoe and the Bayesian Lasso. In Figure 4, we plot the posterior expectations $\mathbb{E}(\mu_i | X_i)$ for the $\text{IGG}_{1/n}$ prior and the posterior expectations $E(\mu_i | X_1, \dots, X_n)$ for the HS and BL priors and the posterior expectations. Figure 4 clearly shows that the noise observations are shrunk towards zero for the $\text{IGG}_{1/n}$ prior, while the signals are left mostly unshrunk. That is, for the $\text{IGG}_{1/n}$ prior, the amount of posterior shrinkage (or the difference between the 45° line and the posterior expectation) is negligibly small for observations that are far away from zero. In comparison to the horseshoe, there seems to be slightly more shrinkage towards zero for the observations near zero under the $\text{IGG}_{1/n}$ prior. Under the assumption of sparsity, this is not a problem because most of the true θ_i ’s are in fact equal to zero. On the other hand, Figure 4 shows that the Bayesian Lasso

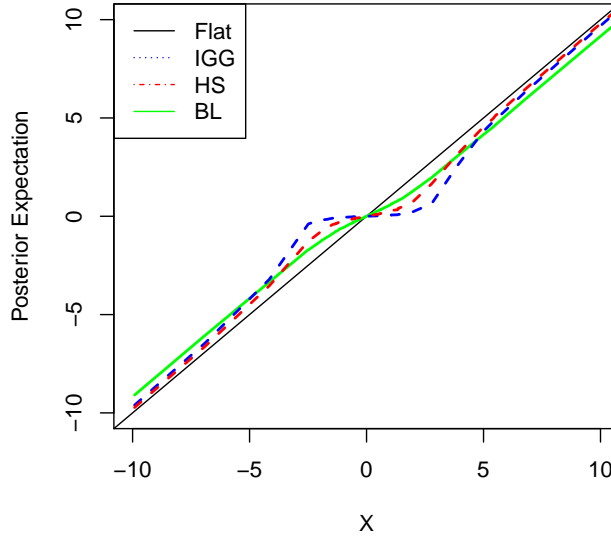


Figure 4: Posterior Mean $\mathbb{E}(\mu|X)$ vs. X plot for $p = 0.25$.

tends to undershrink noise and overshrink signals, which explains its inferior performance to the $\text{IGG}_{1/n}$ prior.

7 Concluding Remarks

In this paper, we have introduced a new scale-mixture shrinkage prior called the Inverse Gamma-Gamma prior for estimating sparse normal mean vectors. This prior has been shown to have a number of good theoretical properties, including heavy probability mass around zero and heavy tails. This enables the IGG prior to perform selective shrinkage and to attain (near) minimax contraction around the true θ in (1), possibly up to a multiplicative constant. Moreover, by thresholding the posterior mean, the IGG can be used to identify signals in θ . We have investigated the asymptotic risk properties of this classification rule within the decision theoretic framework of Bogdan et al. [8] and established asymptotically optimal theoretical properties for multiple testing. Finally, our simulations demonstrate the IGG's strong finite sample performance for obtaining sparse estimates of θ and for correctly classifying entries in θ as either signals or noise. By setting the hyperparameter $b = \frac{1}{n}$, the IGG prior outperforms other popular shrinkage estimators such as the Dirichlet-Laplace and the horseshoe. In some cases, e.g. when θ is more dense, the $\text{IGG}_{1/n}$ performs significantly better than

its main competitors.

In recent years, Bayesian scale-mixture shrinkage priors have gained a great amount of attention because of their computational efficiency and their ability to mimic point-mass mixtures in obtaining sparse estimates. Our paper contributes to this methodological work. The theory on *fully* Bayesian normal scale-mixture models, however, has been rather sparse, and our paper addresses this theoretical gap. For example, our paper appears to be only the second one to show that a fully Bayesian scale mixture shrinkage prior can attain the (near) minimax rate of posterior contraction. In the context of multiple testing, our paper also appears to be the first one to study theoretical properties of a classification rule based on a fully Bayesian normal scale-mixture shrinkage prior within the ABOS framework of Bogdan et al. [8]. The fully Bayesian formulation of the IGG prior is particularly appealing and beneficial because it does not require the estimation of any tuning parameters through cross-validation or empirical Bayes.

There are a few possible future directions for research. For example, the IGG prior can be adapted to other statistical problems such as sparse covariance estimation, variable selection with covariates, and many others. We could also investigate if the IGG prior can be generalized to a wider family of priors, either by replacing one of the densities on λ or τ or by widening the class of prior densities that are allowed on λ and τ . For example, Ghosh et al. [18] and Ghosh and Chakrabarti [17] examined a very wide class of shrinkage priors that contain a slowly-varying function in one of the hyperprior densities. It would be very interesting to see if a wider family of priors can be generated from our work and whether or not this family enjoys the same robust theoretical properties and strong finite sample performance as the IGG prior.

8 Acknowledgments

The authors would like to thank Dr. Anirban Bhattacharya and Dr. Xueying Tang for sharing their codes, which were modified to generate Figures 1-4.

A Proofs for Section 2 and 3

Proof of Proposition 1. The joint distribution of the prior is proportional to

$$\pi(\theta, \tau, \lambda) \propto (\lambda\tau)^{-1/2} \exp\left(-\frac{\theta^2}{2\lambda\tau}\right) \lambda^{-a-1} \exp\left(-\frac{c}{\lambda}\right) \tau^{b-1} \exp(-c\tau)$$

$$\propto \tau^{b-3/2} \exp(-c\tau) \lambda^{-a-3/2} \exp\left(-\left(\frac{\theta^2}{2\tau} + c\right) \frac{1}{\lambda}\right).$$

Thus,

$$\begin{aligned} \pi(\theta, \tau) &\propto \tau^{b-3/2} \exp(-c\tau) \int_{\lambda=0}^{\infty} \lambda^{-a-3/2} \exp\left(-\left(\frac{\theta^2}{2\tau} + c\right) \frac{1}{\lambda}\right) d\lambda \\ &\propto \left(\frac{\theta^2}{2\tau} + c\right)^{-(a+1/2)} \tau^{b-3/2} e^{-c\tau}, \end{aligned}$$

and thus, the marginal density of θ is proportional to

$$\pi(\theta) \propto \int_{\tau=0}^{\infty} \left(\frac{\theta^2}{2\tau} + c\right)^{-(a+1/2)} \tau^{b-3/2} e^{-c\tau} d\tau. \quad (31)$$

As $|\theta| \rightarrow 0$, the expression in (31) is bounded below by

$$C \int_{\tau=0}^{\infty} \tau^{b-3/2} e^{-c\tau} d\tau, \quad (32)$$

where C is a constant that depends on a , b , and c . The integral expression in (32) clearly diverges to ∞ for any $0 < b < 1/2$. Therefore, (31) diverges to infinity as $|\theta| \rightarrow 0$, by the monotone convergence theorem. \square

Proof of Theorem 1. Since marginally, $X_i | (\lambda_i, \tau_i) \sim N(0, 1 + \lambda_i \tau_i)$, we have

$$\pi(\lambda_i, \tau_i | X_i) \propto \exp\left(-\frac{X_i^2}{2(1 + \lambda_i \tau_i)}\right) \left(\frac{1}{1 + \lambda_i \tau_i}\right)^{1/2} \times \pi(\lambda_i) \times \tilde{\pi}(\tau_i). \quad (33)$$

Since $\kappa_i = \frac{1}{1 + \lambda_i \tau_i}$, we have $\lambda_i = \tau_i^{-1} \left(\frac{1 - \kappa_i}{\kappa_i}\right)$. Consider the bivariate transformation,

$$(\lambda_i, \tau_i) \mapsto (\kappa_i, \tau_i).$$

Then $\frac{\partial \lambda_i}{\partial \kappa_i} = -\tau_i^{-1} \kappa_i^{-2}$, and the Jacobian of the bivariate random variable (κ, τ_i) is given by

$$J = \begin{bmatrix} \frac{\partial \lambda_i}{\partial \kappa_i} & \frac{\partial \lambda_i}{\partial \tau_i} \\ \frac{\partial \tau_i}{\partial \kappa_i} & \frac{\partial \tau_i}{\partial \tau_i} \end{bmatrix},$$

with $|\det(J)| = \tau_i^{-1} \kappa_i^{-2}$.

Therefore, we have from (33) that

$$\pi(\kappa_i, \tau_i | X_i) \propto \exp\left(-\frac{\kappa_i X_i^2}{2}\right) \kappa_i^{1/2} \tau_i^{-1} \kappa_i^{-2} \times \pi\left(\tau_i^{-1} \left(\frac{1 - \kappa_i}{\kappa_i}\right)\right) \times \tilde{\pi}(\tau_i)$$

$$\begin{aligned}
& \propto \exp\left(-\frac{\kappa_i X_i^2}{2}\right) \tau_i^{-1} \kappa_i^{-3/2} \times \tilde{\pi}(\tau_i) \\
& \quad \times \left\{ \left[\tau_i^{-1} \left(\frac{1 - \kappa_i}{\kappa_i} \right) \right]^{-a-1} \exp\left(-\frac{c\kappa_i \tau_i}{1 - \kappa_i}\right) \right\} \\
& \propto \exp\left(-\frac{\kappa_i X_i^2}{2}\right) \kappa_i^{a-1/2} (1 - \kappa_i)^{-a-1} \tau_i^a \exp\left(-\frac{c\kappa_i \tau_i}{1 - \kappa_i}\right) \tilde{\pi}(\tau_i).
\end{aligned}$$

Thus,

$$\begin{aligned}
\pi(\kappa_i | X_i) & \propto \exp\left(-\frac{\kappa_i X_i^2}{2}\right) \kappa_i^{a-1/2} (1 - \kappa_i)^{-a-1} \\
& \quad \times \int_{\tau_i=0}^{\infty} \tau_i^a \exp\left(-\frac{c\kappa_i \tau_i}{1 - \kappa_i}\right) \tilde{\pi}(\tau_i) d\tau_i.
\end{aligned}$$

Now, since $\tau_i \sim \text{Gamma}(b, c)$, $\tilde{\pi}(\tau_i) \propto \tau_i^{b-1} e^{-c\tau_i}$. Thus,

$$\begin{aligned}
\pi(\kappa_i | X_i) & \propto \exp\left(-\frac{\kappa_i X_i^2}{2}\right) \kappa_i^{a-1/2} (1 - \kappa_i)^{-a-1} \\
& \quad \times \int_{\tau_i=0}^{\infty} \tau_i^{a+b-1} \exp\left(-\frac{c\tau_i}{1 - \kappa_i}\right) d\tau_i \\
& \propto \exp\left(-\frac{\kappa_i X_i^2}{2}\right) \kappa_i^{a-1/2} (1 - \kappa_i)^{-a-1} \left[\frac{c}{1 - \kappa_i} \right]^{-(a+b)} \\
& \propto \exp\left(-\frac{\kappa_i X_i^2}{2}\right) \kappa_i^{a-1/2} (1 - \kappa_i)^{b-1}, \quad \kappa_i \in (0, 1).
\end{aligned}$$

□

Proof of Theorem 2. Since $\exp\left(-\frac{\kappa_i X_i^2}{2}\right)$ is strictly decreasing in κ_i on $(0, 1)$, we have

$$\begin{aligned}
\mathbb{E}(1 - \kappa_i | X_i) & = \frac{\int_0^1 \kappa_i^{a-1/2} (1 - \kappa_i)^{b-1} \exp\left(-\frac{\kappa_i X_i^2}{2}\right) d\kappa_i}{\int_0^1 \kappa_i^{a-1/2} (1 - \kappa_i)^{b-1} \exp\left(-\frac{\kappa_i X_i^2}{2}\right) d\kappa_i} \\
& \leq \frac{e^{X_i^2/2} \int_0^1 \kappa_i^{a-1/2} (1 - \kappa_i)^{b-1} d\kappa_i}{\int_0^1 \kappa_i^{a-1/2} (1 - \kappa_i)^{b-1} d\kappa_i}
\end{aligned}$$

$$\begin{aligned}
&= e^{X_i^2/2} \frac{\Gamma(a+1/2)\Gamma(b_n+1)}{\Gamma(a+b_n+3/2)} \times \frac{\Gamma(a+b_n+1/2)}{\Gamma(a+1/2)\Gamma(b_n)} \\
&= e^{X_i^2/2} \left(\frac{b_n}{a+b_n+1/2} \right).
\end{aligned}$$

□

Proof of Theorem 3. Note that since $a \in (\frac{1}{2}, \infty)$, $\kappa_i^{a-1/2}$ is increasing in κ_i on $(0, 1)$. Additionally, since $b_n \in (0, 1)$, $(1 - \kappa_i)^{b_n-1}$ is increasing in κ_i on $(0, 1)$. Using these facts, we have

$$\begin{aligned}
P(\kappa_i < \epsilon | X_i) &\leq \frac{\int_0^\epsilon \exp\left(-\frac{\kappa_i X_i^2}{2}\right) \kappa_i^{a-1/2} (1 - \kappa_i)^{b_n-1} d\kappa_i}{\int_\epsilon^1 \exp\left(-\frac{\kappa_i X_i^2}{2}\right) \kappa_i^{a-1/2} (1 - \kappa_i)^{b_n-1} d\kappa_i} \\
&\leq \frac{e^{X_i^2/2} \int_0^\epsilon \kappa_i^{a-1/2} (1 - \kappa_i)^{b_n-1} d\kappa_i}{\int_\epsilon^1 \kappa_i^{a-1/2} (1 - \kappa_i)^{b_n-1} d\kappa_i} \\
&\leq \frac{e^{X_i^2/2} (1 - \epsilon)^{b_n-1} \int_0^\epsilon \kappa_i^{a-1/2} d\kappa_i}{\epsilon^{a-1/2} \int_\epsilon^1 (1 - \kappa_i)^{b_n-1} d\kappa_i} \\
&= \frac{e^{X_i^2/2} (1 - \epsilon)^{b_n-1} \left(a + \frac{1}{2}\right)^{-1} \epsilon^{a+1/2}}{b_n^{-1} \epsilon^{a-1/2} (1 - \epsilon)^b} \\
&= e^{X_i^2/2} \frac{b_n \epsilon}{(a + 1/2) (1 - \epsilon)}.
\end{aligned}$$

□

Proof of Theorem 4. First, note that since $b_n \in (0, 1)$, $(1 - \kappa_i)^{b_n-1}$ is increasing in κ_i on $(0, 1)$. Therefore, letting C denote the normalizing constant that depends on X_i , we have

$$\begin{aligned}
\int_0^\eta \pi(\kappa_i | X_i) d\kappa_i &= C \int_0^\eta \exp\left(-\frac{\kappa_i X_i^2}{2}\right) \kappa_i^{a-1/2} (1 - \kappa_i)^{b_n-1} d\kappa_i \\
&\geq C \int_0^{\eta^\delta} \exp\left(-\frac{\kappa_i X_i^2}{2}\right) \kappa_i^{a-1/2} (1 - \kappa_i)^{b_n-1} d\kappa_i
\end{aligned}$$

$$\begin{aligned}
&\geq C \exp\left(-\frac{\eta\delta}{2}X_i^2\right) \int_0^{\eta\delta} \kappa_i^{a-1/2} d\kappa_i \\
&= C \exp\left(-\frac{\eta\delta}{2}X_i^2\right) \left(a + \frac{1}{2}\right)^{-1} (\eta\delta)^{a+\frac{1}{2}}.
\end{aligned} \tag{34}$$

Also, since $a \in (\frac{1}{2}, \infty)$, $\kappa_i^{a-1/2}$ is increasing in κ_i on $(0, 1)$.

$$\begin{aligned}
\int_{\eta}^1 \pi(\kappa_i|X_i) d\kappa_i &= C \int_{\eta}^1 \exp\left(-\frac{\kappa_i X_i^2}{2}\right) \kappa_i^{a-1/2} (1-\kappa_i)^{b_n-1} d\kappa_i \\
&\leq C \exp\left(-\frac{\eta X_i^2}{2}\right) \int_{\eta}^1 \kappa_i^{a-1/2} (1-\kappa_i)^{b_n-1} d\kappa_i \\
&\leq C \exp\left(-\frac{\eta X_i^2}{2}\right) \int_{\eta}^1 (1-\kappa_i)^{b_n-1} d\kappa_i \\
&= C \exp\left(-\frac{\eta X_i^2}{2}\right) b_n^{-1} (1-\eta)^{b_n}.
\end{aligned} \tag{35}$$

Combining (34) and (35), we have

$$\begin{aligned}
P(\kappa_i > \eta|X_i) &\leq \frac{\int_{\eta}^1 \pi(\kappa_i|X_i) d\kappa_i}{\int_0^{\eta} \pi(\kappa_i|X_i) d\kappa_i} \\
&\leq \frac{\left(a + \frac{1}{2}\right) (1-\eta)^{b_n}}{b_n (\eta\delta)^{a+\frac{1}{2}}} \exp\left(-\frac{\eta(1-\delta)}{2}X_i^2\right).
\end{aligned}$$

□

B Proofs for Section 4

Before proving Theorems 5 and Theorem 6, we first state two lemmas. For both Lemmas 1 and 2, we denote $T(x) = \{\mathbb{E}(1-\kappa)|x\}x$ as the posterior mean under (9) for a single observation x , where $\kappa = \frac{1}{1+\lambda\tau}$. Our arguments follow closely those of van der Pas et al. [32] and Ghosh and Chakrabarti [17], except that their arguments rely on controlling the rate of decay of tuning parameter τ or an empirical Bayes estimator $\hat{\tau}$. In our case, since we are dealing with a fully Bayesian model, the degree of posterior contraction is instead controlled by the positive sequence of hyperparameters b_n in (9).

Lemma 1. Let $T(x)$ be the posterior mean under (9) for a single observation x drawn from $N(\theta, 1)$. Suppose we have constants $\eta \in (0, \frac{1}{2})$, $\delta \in (0, 1)$, $a \in (\frac{1}{2}, \infty)$, and $b_n \in (0, 1)$, where $b_n \rightarrow 0$ as $n \rightarrow \infty$. Then for any $d > 2$ and fixed n , $|T(x) - x|$ can be bounded above by a real-valued function $h_n(x)$, depending on d and satisfying the following:

For any $\rho > d$, $h_n(\cdot)$ satisfies

$$\lim_{n \rightarrow \infty} \sup_{|x| > \sqrt{\rho \log(\frac{1}{b_n})}} h_n(x) = 0. \quad (36)$$

Proof of Lemma 1. Fix $\eta \in (0, 1)$, $\delta \in (0, 1)$. First observe that

$$\begin{aligned} |T(x) - x| &= |x \mathbb{E}(\kappa | x)| \\ &\leq |x \mathbb{E}(\kappa 1\{\kappa < \eta\})| + |x \mathbb{E}(\kappa 1\{\kappa > \eta\})|. \end{aligned} \quad (37)$$

We consider the two terms in (37) separately. From (11) and the fact that $(1 - \kappa)^{b_n - 1}$ is increasing in $\kappa \in (0, 1)$ when $b_n \in (0, 1)$, we have

$$\begin{aligned} |x \mathbb{E}(\kappa 1\{\kappa < \eta\})| &= \left| x \frac{\int_0^\eta \kappa \cdot \kappa^{a-1/2} (1 - \kappa)^{b_n-1} e^{-\kappa x^2/2} d\kappa}{\int_0^1 \kappa^{a-1/2} (1 - \kappa)^{b_n-1} e^{-\kappa x^2/2} d\kappa} \right| \\ &\leq |x| \left| (1 - \eta)^{b_n-1} \frac{\int_0^\eta \kappa^{a+1/2} e^{-\kappa x^2/2} d\kappa}{\int_0^1 \kappa^{a-1/2} e^{-\kappa x^2/2} d\kappa} \right| \\ &= (1 - \eta)^{b_n-1} \left| \frac{\int_0^{\eta x^2} \left(\frac{t}{x^2}\right)^{a+1/2} e^{-t/2} dt}{\int_0^{x^2} \left(\frac{t}{x^2}\right)^{a-1/2} e^{-t/2} dt} \right| |x| \\ &= (1 - \eta)^{b_n-1} \left| \frac{1}{x^2} \frac{\int_0^{\eta x^2} t^{a+1/2} e^{-t/2} dt}{\int_0^{x^2} t^{a-1/2} e^{-t/2} dt} \right| |x| \\ &\leq (1 - \eta)^{b_n-1} \left| \frac{\int_0^\infty t^{a+1/2} e^{-t/2} dt}{\int_0^{x^2} t^{a-1/2} e^{-t/2} dt} \right| |x|^{-1} \\ &= C(n) \left[\left| \int_0^{x^2} t^{a-1/2} e^{-t/2} dt \right| \right]^{-1} |x|^{-1} \\ &= h_1(x) \quad (\text{say}), \end{aligned} \quad (38)$$

where we use a change of variables $t = \kappa x^2$ in the second equality, and

$$C(n) = (1 - \eta)^{b_n-1} \left(\frac{\Gamma(1)\Gamma(a+3/2)}{\Gamma(a+5/2)} \right) = (1 - \eta)^{b_n-1} \left(a + \frac{3}{2} \right)^{-1}.$$

Next, we observe that since $\kappa \in (0, 1)$,

$$|x \mathbb{E}(\kappa 1\{\kappa > \eta\})| \leq |x P(\kappa > \eta | x)|$$

$$\begin{aligned}
&\leq \frac{\left(a + \frac{1}{2}\right)(1-\eta)^{b_n}}{b_n(\eta\delta)^{a+1/2}}|x| \exp\left(-\frac{\eta(1-\delta)}{2}x^2\right) \\
&= h_2(x) \quad (\text{say}),
\end{aligned} \tag{39}$$

where we use Theorem 4 for the second inequality.

Let $h_n(x) = h_1(x) + h_2(x)$. Combining (37)-(39), we have that for every $x \in \mathbb{R}$ and fixed n ,

$$|T(x) - x| \leq h_n(x), \tag{40}$$

Observe from (38) that for fixed n , $h_1(x)$ is strictly decreasing in $|x|$. Therefore, we have that for any fixed n and $\rho > 0$,

$$\sup_{|x| > \sqrt{\rho \log\left(\frac{1}{b_n}\right)}} h_1(x) \leq C(n) \left[\left| \sqrt{\rho \log\left(\frac{1}{b_n}\right)} \int_0^{\rho \log\left(\frac{1}{b_n}\right)} t^{a-1/2} e^{-t/2} dt \right| \right]^{-1},$$

and since $b_n \rightarrow 0$ as $n \rightarrow \infty$, this implies that

$$\lim_{n \rightarrow \infty} \sup_{|x| > \sqrt{\rho \log\left(\frac{1}{b_n}\right)}} h_1(x) = 0. \tag{41}$$

Next, observe that from (39) that for fixed n , $h_2(x)$ is eventually decreasing in $|x|$ with a maximum when $|x| = \frac{1}{\sqrt{\eta(1-\delta)}}$. Therefore, for sufficiently large n , we have

$$\sup_{|x| > \sqrt{\rho \log\left(\frac{1}{b_n}\right)}} h_2(x) \leq h_2\left(\sqrt{\rho \log\left(\frac{1}{b_n}\right)}\right).$$

Letting $K \equiv K(a, \eta, \delta) = \frac{(a+\frac{1}{2})}{(\eta\delta)^{a+1/2}}$, we have from (39) and the fact that $0 < b_n < 1$ for all n that

$$\begin{aligned}
\lim_{n \rightarrow \infty} h_2\left(\sqrt{\rho \log\left(\frac{1}{b_n}\right)}\right) &= K \lim_{n \rightarrow \infty} \frac{(1-\eta)^{b_n}}{b_n} \sqrt{\rho \log\left(\frac{1}{b_n}\right)} e^{-\frac{\eta(1-\delta)}{2} \rho \log\left(\frac{1}{b_n}\right)} \\
&\leq K \lim_{n \rightarrow \infty} \frac{1}{b_n} \sqrt{\rho \log\left(\frac{1}{b_n}\right)} e^{\frac{\eta(1-\delta)}{2} \log(b_n^\rho)} \\
&= K \sqrt{\rho} \lim_{n \rightarrow \infty} (b_n)^{\frac{\eta(1-\delta)}{2} (\rho - \frac{2}{\eta(1-\delta)})} \sqrt{\log\left(\frac{1}{b_n}\right)} \\
&= \begin{cases} 0 & \text{if } \rho > \frac{2}{\eta(1-\delta)}, \\ \infty & \text{otherwise,} \end{cases}
\end{aligned}$$

from which it follows that

$$\lim_{n \rightarrow \infty} \sup_{|x| > \sqrt{\rho \log(\frac{1}{b_n})}} h_2(x) = \begin{cases} 0 & \text{if } \rho > \frac{2}{\eta(1-\delta)}, \\ \infty & \text{otherwise.} \end{cases} \quad (42)$$

Combining (41) and (42), we have for $h_n(x) = h_1(x) + h_2(x)$ that

$$\lim_{n \rightarrow \infty} \sup_{|x| > \sqrt{\rho \log(\frac{1}{b_n})}} h_n(x) = \begin{cases} 0 & \text{if } \rho > \frac{2}{\eta(1-\delta)}, \\ \infty & \text{otherwise.} \end{cases} \quad (43)$$

Since $\eta \in (0, 1)$, $\delta \in (0, 1)$, it is clear that any real number larger than 2 can be expressed in the form $\frac{2}{\eta(1-\delta)}$. For example, taking $\eta = \frac{5}{6}$ and $\delta = \frac{1}{5}$, we obtain $\frac{2}{\eta(1-\delta)} = 3$. Hence, given any $d > 2$, choose $0 < \eta, \delta < 1$ such that $c = \frac{2}{\eta(1-\delta)}$. Clearly, $h_n(\cdot)$ depends on d . Following (40) and (43), we see that $|T(x) - x|$ is uniformly bounded above by $h_n(x)$ for all n and $d > 2$ and that condition (36) is also satisfied when $d > 2$. This completes the proof. \square

Remark: Under the conditions of Lemma 1, we see that for any fixed n ,

$$\lim_{|x| \rightarrow \infty} |T(x) - x| = 0. \quad (44)$$

Equation (44) shows that for the IGG prior, large observations almost remain unshrunk no matter what the sample size n is. This is critical to its ability to properly identify signals in our data. We now present our second lemma which bounds the posterior variance.

Lemma 2. *Let $T(x_i)$ be the posterior mean under (9). Then for a single observation $x \sim N(\theta, 1)$, the posterior variance $\text{Var}(\theta|x)$ can be bounded above by*

$$\text{Var}(\theta|x) \leq 1 - (T(x) - x)^2 + x^2, \quad (45)$$

and

$$\text{Var}(\theta|x) \leq 1 - T(x)^2 + x^2. \quad (46)$$

Proof of Lemma 2. We first prove (45). By the law of the iterated variance and the fact that $\theta|\kappa, x \sim N((1 - \kappa)x, 1 - \kappa)$, we have

$$\begin{aligned} \text{Var}(\theta|x) &= \mathbb{E}[\text{Var}(\theta|\kappa, x)] + \text{Var}[\mathbb{E}(\theta|\kappa, x)] \\ &= \mathbb{E}(1 - \kappa|x) + \text{Var}[(1 - \kappa)x|x] \end{aligned}$$

$$\begin{aligned}
&= \mathbb{E}(1 - \kappa|x) + x^2 \text{Var}(\kappa|x) \\
&= \mathbb{E}[(1 - \kappa|x) + x^2 \mathbb{E}(\kappa^2|x) - x^2 [\mathbb{E}(\kappa|x)]^2].
\end{aligned}$$

Since $x - T(x) = x\mathbb{E}(\kappa|x)$, we rewrite the above as

$$\begin{aligned}
\text{Var}(\theta|x) &= \frac{T(x)}{x} - (T(x) - x)^2 + x^2 \frac{\int_0^1 \kappa^{a+3/2} (1 - \kappa)^{b_n-1} e^{-\kappa x^2/2} dx}{\int_0^1 \kappa^{a+1/2} (1 - \kappa)^{b_n-1} e^{-\kappa x^2/2} dx} \\
&\leq 1 - (T(x) - x)^2 + x^2,
\end{aligned}$$

where the inequality follows from the fact that $\kappa \in (0, 1)$, so $\kappa^{a+\frac{3}{2}} \leq \kappa^{a+\frac{1}{2}}$ for all $a \in \mathbb{R}$.

Next, we show that (46) holds. We may alternatively represent $\text{Var}(\theta|x)$ as

$$\begin{aligned}
\text{Var}(\theta|x) &= \mathbb{E}(1 - \kappa|x) + x^2 \mathbb{E}[(1 - \kappa)^2|x] - x^2 \mathbb{E}^2[(1 - \kappa)|x] \\
&= \frac{T(x)}{x} - T(x)^2 + x^2 \frac{\int_0^1 \kappa^{a+1/2} (1 - \kappa)^{b_n+1} e^{-\kappa x^2/2} dx}{\int_0^1 \kappa^{a+1/2} (1 - \kappa)^{b_n-1} e^{-\kappa x^2/2} dx} \\
&\leq 1 - T(x)^2 + x^2,
\end{aligned}$$

where the final inequality holds because $(1 - \kappa)^{b_n+1} \leq (1 - \kappa)^{b_n-1}$ for all $b_n \in \mathbb{R}$ when $\kappa \in (0, 1)$. \square

Lemmas 1 and 2 are crucial in proving Theorems 5 and 6, which provide asymptotic upper bounds on the mean squared error (MSE) for the posterior mean under the IGG_n prior (9) and the posterior variance under (9). These theorems will ultimately allow us to provide sufficient conditions under which the posterior mean and posterior distribution under the IGG_n prior contract at minimax rates.

Proof of Theorem 5. Define $\tilde{q}_n = \#\{i : \theta_{0i} \neq 0\}$. We split the MSE $\mathbb{E}_{\theta_0} \|T(\mathbf{X}) - \theta_0\|^2 = \sum_{i=1}^n \mathbb{E}_{\theta_{0i}} (T(X_i) - \theta_{0i})^2$ as

$$\sum_{i=1}^n \mathbb{E}_{\theta_{0i}} (T(X_i) - \theta_{0i})^2 = \sum_{i:\theta_{0i} \neq 0} \mathbb{E}_{\theta_{0i}} (T(X_i) - \theta_{0i})^2 + \sum_{i:\theta_{0i}=0} \mathbb{E}_{\theta_{0i}} (T(X_i) - \theta_{0i})^2. \quad (47)$$

We consider the nonzero means and the zero means separately.

Nonzero means: For $\theta_{0i} \neq 0$, using the Cauchy-Schwartz inequality and the fact that $\mathbb{E}_{\theta_{0i}} (X_i - \theta_{0i})^2 = 1$, we get

$$\mathbb{E}_{\theta_{0i}} (T(X_i) - \theta_i)^2 = \mathbb{E}_{\theta_{0i}} (T(X_i) - X_i + X_i - \theta_i)^2$$

$$\begin{aligned}
&= \mathbb{E}_{\theta_{0i}}(T(X_i) - X_i)^2 + \mathbb{E}_{\theta_{0i}}(X_i - \theta_{0i})^2 + 2\mathbb{E}_{\theta_{0i}}(T(X_i) - X_i)(X_i - \theta_{0i}) \\
&\leq \mathbb{E}_{\theta_{0i}}(T(X_i) - X_i)^2 + 1 + 2\sqrt{\mathbb{E}_{\theta_{0i}}(T(X_i) - X_i)^2} \sqrt{\mathbb{E}_{\theta_{0i}}(X_i - \theta_{0i})^2} \\
&= \left[\sqrt{\mathbb{E}_{\theta_{0i}}(T(X_i) - X_i)^2} + 1 \right]^2.
\end{aligned} \tag{48}$$

We now define

$$\zeta_n = \sqrt{2 \log \left(\frac{1}{b_n} \right)}. \tag{49}$$

Let us fix any $d > 2$ and choose any $\rho > 2$. Then, using Lemma 1, there exists a non-negative real-valued function $h_n(\cdot)$, depending on d such that

$$|T_n(x) - x| \leq h_n(x) \text{ for all } x \in \mathbb{R}, \tag{50}$$

and

$$\lim_{n \rightarrow \infty} \sup_{|x| > \rho \zeta_n} h_n(x) = 0. \tag{51}$$

Using the fact that $(T(X_i) - X_i)^2 \leq X_i^2$, together with (51), we obtain

$$\begin{aligned}
\mathbb{E}_{\theta_{0i}}(T(X_i) - X_i)^2 &= \mathbb{E}_{\theta_{0i}}[(T(X_i) - X_i)^2 1\{|X_i| \leq \rho \zeta_n\}] \\
&\quad + \mathbb{E}_{\theta_{0i}}[T(X_i - X_i)^2 1\{|X_i| > \rho \zeta_n\}] \\
&\leq \rho^2 \zeta_n^2 + \left(\sup_{|x| > \rho \zeta_n} h_n(x) \right)^2.
\end{aligned} \tag{52}$$

Using (51) and the fact that $\zeta_n \rightarrow \infty$ as $n \rightarrow \infty$ by (49), it follows that

$$\left(\sup_{|x| > \rho \zeta_n} h_n(x) \right)^2 = o(\zeta_n^2) \text{ as } n \rightarrow \infty. \tag{53}$$

By combining (52) and (53), we get

$$\mathbb{E}_{\theta_{0i}}(T(X_i) - X_i)^2 \leq \rho^2 \zeta_n^2 (1 + o(1)) \text{ as } n \rightarrow \infty. \tag{54}$$

Noting that (54) holds uniformly for any i such that $\theta_{0i} \neq 0$, we combine (48), (49), and (54) to conclude that

$$\sum_{i: \theta_{0i} \neq 0} \mathbb{E}_{\theta_{0i}}(T(X_i) - \theta_{0i})^2 \lesssim \tilde{q}_n \log \left(\frac{1}{b_n} \right), \text{ as } n \rightarrow \infty, \tag{55}$$

Zero means: For $\theta_{0i} = 0$, the corresponding MSE can be split as follows:

$$\mathbb{E}_0 T(X_i)^2 = \mathbb{E}_0 [T(X_i)^2 1\{|X_i| \leq \zeta_n\}] + \mathbb{E}_0 [T(X_i)^2 1\{|X_i| > \zeta_n\}], \quad (56)$$

where ζ_n is as in (49). Using Theorem 2, we have

$$\begin{aligned} \mathbb{E}_0 [T(X_i)^2 1\{|X_i| \leq \zeta_n\}] &\leq \left(\frac{b_n}{a + b_n + 1/2} \right)^2 \int_{-\zeta_n}^{\zeta_n} x^2 e^{x^2/2} dx \\ &\leq \frac{b_n^2}{a^2} \int_{-\zeta_n}^{\zeta_n} x^2 e^{x^2/2} dx \\ &= \frac{2b_n^2}{a^2} \int_0^{\zeta_n} x^2 e^{x^2/2} dx \\ &\leq \frac{2b_n^2}{a} (\zeta_n e^{\zeta_n^2/2}) \\ &\lesssim b_n \sqrt{\log \left(\frac{1}{b_n} \right)}, \end{aligned} \quad (57)$$

where we use the integration by parts for the third inequality.

Now, using the fact that $|T(x)| \leq |x|$ for all $x \in \mathbb{R}$,

$$\begin{aligned} \mathbb{E}_0 [T(X_i)^2 1\{|X_i| > \zeta_n\}] &\leq 2 \int_{\zeta_n}^{\infty} x^2 \phi(x) dx \\ &= 2[\zeta_n \phi(\zeta_n) + 1 - \Phi(\zeta_n)] \\ &\leq 2\zeta_n \phi(\zeta_n) + \frac{2\phi(\zeta_n)}{\zeta_n} \\ &= \sqrt{\frac{2}{\pi}} \zeta_n (e^{-\zeta_n^2/2} + o(1)) \\ &\lesssim b_n \sqrt{\log \left(\frac{1}{b_n} \right)}, \end{aligned} \quad (58)$$

where we used the identity $x^2 \phi(x) = \phi(x) - \frac{d}{dx}[x\phi(x)]$ for the first equality and Mill's ratio $1 - \Phi(x) \leq \frac{\phi(x)}{x}$ for all $x > 0$ in the second inequality. Combining (57)-(58), we have that

$$\sum_{i:\theta_{0i}=0} \mathbb{E}_{\theta_{0i}} T(X_i)^2 \lesssim (n - \tilde{q}_n) b_n \sqrt{\log \left(\frac{1}{b_n} \right)}. \quad (59)$$

From (47), (55) and (59), it immediately follows that

$$\mathbb{E} \|T(\mathbf{X}) - \boldsymbol{\theta}_0\|^2 = \sum_{i=1}^n \mathbb{E}_{\theta_{0i}} (T(X_i) - \theta_{0i})^2$$

$$\lesssim \tilde{q}_n \log\left(\frac{1}{b_n}\right) + (n - \tilde{q}_n)b_n \sqrt{\log\left(\frac{1}{b_n}\right)}.$$

The required result now follows by observing that $\tilde{q}_n \leq q_n$ and $q_n = o(n)$ and then taking the supremum over all $\boldsymbol{\theta}_0 \in \ell_0[q_n]$. This completes the proof of Theorem 5. \square

Proof of Theorem 6. Define $\tilde{q}_n = \#\{i : \theta_{0i} \neq 0\}$. We decompose the total variance as

$$\mathbb{E}_{\boldsymbol{\theta}_0} \sum_{i=1}^n \text{Var}(\theta_{0i}|X_i) = \sum_{i:\theta_{0i} \neq 0} \mathbb{E}_{\theta_{0i}} \text{Var}(\theta_{0i}|X_i) + \sum_{i:\theta_{0i}=0} \mathbb{E}_{\theta_{0i}} \text{Var}(\theta_{0i}|X_i), \quad (60)$$

and consider the nonzero means and zero means separately.

Nonzero means: For $\theta_{0i} \neq 0$, we have

$$\begin{aligned} \mathbb{E}_{\theta_{0i}} \text{Var}(\theta_{0i}|X_i) &\leq \mathbb{E}_{\theta_{0i}} [1 - (T(X_i) - X_i)^2 + X_i^2] \\ &\leq 2 + \mathbb{E}_{\theta_{0i}} (T(X_i) - X_i)^2 \\ &\lesssim \log\left(\frac{1}{b_n}\right), \end{aligned} \quad (61)$$

where the first inequality follows from (45) in Lemma 2 and the last one follows from (54).

Zero means: For $\theta_{0i} = 0$, we have

$$\begin{aligned} \mathbb{E}_0 \text{Var}(\theta_{0i}|X_i) &\leq \mathbb{E}_0 [1 - T(X_i)^2 + X_i^2] \\ &\leq 2 + \mathbb{E}_0 T(X_i)^2 \\ &\lesssim b_n \sqrt{\log\left(\frac{1}{b_n}\right)}, \end{aligned} \quad (62)$$

where the first inequality follows from (46) in Lemma 2 and the last one follows from (56)-(58). Combining (60)-(62), we get

$$\mathbb{E}_{\boldsymbol{\theta}_0} \text{Var}(\theta_{0i}|X_i) \lesssim \tilde{q}_n \log\left(\frac{1}{b_n}\right) + (n - \tilde{q}_n)b_n \sqrt{\log\left(\frac{1}{b_n}\right)}.$$

The required result now follows by observing that $\tilde{q}_n \leq q_n$ and $q_n = o(n)$ and then taking the supremum over all $\boldsymbol{\theta}_0 \in \ell_0[q_n]$. This completes the proof of Theorem 6. \square

C Proofs for Section 5

To establish conditions for (28) to hold, we must first find bounds on the Type I and Type II error probabilities, t_{1i} and t_{2i} respectively, for rule (27). These error probabilities are given respectively by

$$\begin{aligned} t_{1i} &= P \left[\mathbb{E}(1 - \kappa_i | X_i) > \frac{1}{2} \middle| H_{0i} \text{ is true} \right], \\ t_{2i} &= P \left[\mathbb{E}(1 - \kappa_i | X_i) \leq \frac{1}{2} \middle| H_{1i} \text{ is true} \right]. \end{aligned} \quad (63)$$

To this end, we first prove the following lemmas, Lemma 3-6 which give upper and lower bounds for t_{1i} and t_{2i} in (63).

Lemma 3. *Suppose that X_1, \dots, X_n are i.i.d. observations having distribution (21) where the sequence of vectors (ψ^2, p) satisfies Assumption 1. Suppose we wish to test (22) using the classification rule (27). Then for all n , an upper bound for the probability of a Type I error for the i th test is given by*

$$t_{1i} \leq \frac{2b_n}{\sqrt{\pi}(a + b_n + 1/2)} \left[\log \left(\frac{a + b_n + 1/2}{2b_n} \right) \right]^{-1/2}.$$

Proof of Lemma 3. By Theorem 2, the event $\left\{ \mathbb{E}(1 - \kappa_i | X_i) > \frac{1}{2} \right\}$ implies the event

$$\begin{aligned} &\left\{ e^{X_i^2/2} \left(\frac{b_n}{a + b_n + 1/2} \right) > \frac{1}{2} \right\} \\ &\Leftrightarrow \left\{ X_i^2 > 2 \log \left(\frac{a + b_n + 1/2}{2b_n} \right) \right\}. \end{aligned}$$

Therefore, noting that under H_{0i} , $X_i \sim N(0, 1)$ and using Mill's ratio, i.e. $P(|Z| > x) \leq \frac{2\phi(x)}{x}$, we have

$$\begin{aligned} t_{1i} &\leq P \left(X_i^2 > 2 \log \left(\frac{a + b_n + 1/2}{2b_n} \right) \middle| H_{0i} \text{ is true} \right) \\ &= P \left(|Z| > \sqrt{2 \log \left(\frac{a + b_n + 1/2}{2b_n} \right)} \right) \\ &\leq \frac{2\phi \left(\sqrt{2 \log \left(\frac{a + b_n + 1/2}{2b_n} \right)} \right)}{\sqrt{2 \log \left(\frac{a + b_n + 1/2}{2b_n} \right)}} \end{aligned}$$

$$= \frac{2b_n}{\sqrt{\pi}(a + b_n + 1/2)} \left[\log \left(\frac{a + b_n + 1/2}{2b_n} \right) \right]^{-1/2}.$$

□

Lemma 4. Suppose that X_1, \dots, X_n are i.i.d. observations having distribution (21) where the sequence of vectors (ψ^2, p) satisfies Assumption 1. Suppose we wish to test (22) using the classification rule (27). Suppose further that $a \in (\frac{1}{2}, \infty)$ and $b_n \in (0, 1)$, with $b_n \rightarrow 0$ as $n \rightarrow \infty$. Then for any $\eta \in (0, \frac{1}{2})$, $\delta \in (0, 1)$, and sufficiently large n , a lower bound for the probability of a Type I error for the i th test is given by

$$t_{1i} \geq 1 - \Phi \left(\sqrt{\frac{2}{\eta(1-\delta)} \left[\log \left(\frac{(a + \frac{1}{2})(1-\eta)^{b_n}}{b_n(\eta\delta)^{a+\frac{1}{2}}}} \right) \right]} \right).$$

Proof of Lemma 4. By definition, the probability of a Type I error for the i th decision is given by

$$t_{1i} = P \left[\mathbb{E}(1 - \kappa_i | X_i) > \frac{1}{2} \mid H_{0i} \text{ is true} \right].$$

We have by Theorem 4 that

$$\mathbb{E}(\kappa_i | X_i) \leq \eta + \frac{(a + \frac{1}{2})(1-\eta)^{b_n}}{b_n(\eta\delta)^{a+\frac{1}{2}}} \exp \left(-\frac{\eta(1-\delta)}{2} X_i^2 \right),$$

and so it follows that

$$\left\{ \mathbb{E}(1 - \kappa_i | X_i) > \frac{1}{2} \right\} \supseteq \left\{ \frac{(a + \frac{1}{2})(1-\eta)^{b_n}}{b_n(\eta\delta)^{a+\frac{1}{2}}} \exp \left(-\frac{\eta(1-\delta)}{2} X_i^2 \right) < \frac{1}{2} - \eta \right\}.$$

Thus, using the definition of t_{1i} and the above and noting that under H_{0i} , $X_i \sim N(0, 1)$, as $n \rightarrow \infty$,

$$\begin{aligned} t_{1i} &\geq P \left(\frac{(a + \frac{1}{2})(1-\eta)^{b_n}}{b_n(\eta\delta)^{a+\frac{1}{2}}} \exp \left(-\frac{\eta(1-\delta)}{2} X_i^2 \right) < \frac{1}{2} - \eta \mid H_{0i} \text{ is true} \right) \\ &= P \left(X_i^2 > \frac{2}{\eta(1-\delta)} \left[\log \left(\frac{(a + \frac{1}{2})(1-\eta)^{b_n}}{b_n(\eta\delta)^{a+\frac{1}{2}} (\frac{1}{2} - \eta)} \right) \right] \right) \end{aligned}$$

$$\begin{aligned}
&= 2P \left(Z > \sqrt{\frac{2}{\eta(1-\delta)} \left[\log \left(\frac{\left(a + \frac{1}{2}\right) (1-\eta)^{b_n}}{b_n(\eta\delta)^{a+\frac{1}{2}} \left(\frac{1}{2} - \eta\right)} \right) \right]} \right) \\
&= 2 \left(1 - \Phi \left(\sqrt{\frac{2}{\eta(1-\delta)} \left[\log \left(\frac{\left(a + \frac{1}{2}\right) (1-\eta)^{b_n}}{b_n(\eta\delta)^{a+\frac{1}{2}} \left(\frac{1}{2} - \eta\right)} \right) \right]} \right) \right),
\end{aligned}$$

where for the last inequality, we used the fact that $b_n \rightarrow 0$ as $n \rightarrow \infty$, and the fact that $\eta, \eta\delta \in (0, \frac{1}{2})$, so that the $\log(\cdot)$ term in final equality is greater than zero for sufficiently large n . \square

Lemma 5. *Suppose we have the same set-up as Lemma 4. Assume further that $b_n \rightarrow 0$ in such a way that $\lim_{n \rightarrow \infty} \frac{b_n^{1/4}}{p_n} \in (0, \infty)$. Then for any $\eta \in (0, \frac{1}{2})$, $\delta \in (0, 1)$, and sufficiently large n , an upper bound for the probability of a Type II error for the i th test is given by*

$$t_{2i} \leq \left[2\Phi \left(\sqrt{\frac{C}{2\eta(1-\delta)}} \right) - 1 \right] (1 + o(1)),$$

where the $o(1)$ terms tend to zero as $n \rightarrow \infty$.

Proof of Lemma 5. By definition, the probability of a Type II error is given by

$$t_{2i} = P \left(\mathbb{E}(1 - \kappa_i) \leq \frac{1}{2} \middle| H_{1i} \text{ is true} \right).$$

Fix $\eta \in (0, \frac{1}{2})$ and $\delta \in (0, 1)$. Using the inequality,

$$\kappa_i \leq 1 \{ \eta < \kappa_i \leq 1 \} + \eta,$$

we obtain

$$\mathbb{E}(\kappa_i | X_i) \leq P(\kappa_i > \eta | X_i) + \eta.$$

Coupled with Theorem 4, we obtain that for sufficiently large n ,

$$\left\{ \mathbb{E}(\kappa_i | X_i) > \frac{1}{2} \right\} \subseteq \left\{ \frac{\left(a + \frac{1}{2}\right) (1-\eta)^{b_n}}{b_n(\eta\delta)^{a+\frac{1}{2}}} \exp \left(-\frac{\eta(1-\delta)}{2} X_i^2 \right) > \frac{1}{2} - \eta \right\}.$$

Therefore,

$$t_{2i} = P \left(\mathbb{E}(\kappa_i | X_i) > \frac{1}{2} \middle| H_{1i} \text{ is true} \right)$$

$$\begin{aligned}
&\leq P \left(\frac{\left(a + \frac{1}{2}\right) (1 - \eta)^{b_n}}{b(\eta\delta)^{a_n + \frac{1}{2}}} \exp \left(-\frac{\eta(1 - \delta)}{2} X_i^2 \right) > \frac{1}{2} - \eta \middle| H_{1i} \text{ is true} \right) \\
&= P \left(X_i^2 < \frac{2}{\eta(1 - \delta)} \left\{ \log \left(\frac{a + \frac{1}{2}}{b_n(\eta\delta)^a} \right) - \right. \right. \\
&\quad \left. \left. \log \left(\frac{\left(\frac{1}{2} - \eta\right) (\eta\delta)^{1/2}}{(1 - \eta)^{b_n}} \right) \right\} \middle| H_{1i} \text{ is true} \right) \\
&= P \left(X_i^2 < \frac{2}{\eta(1 - \delta)} \log \left(\frac{a}{b_n(\eta\delta)^a} \right) (1 + o(1)) \middle| H_{1i} \text{ is true} \right), \quad (64)
\end{aligned}$$

where in the final equality, we used the fact that $b_n \rightarrow 0$ as $n \rightarrow \infty$, so the second $\log(\cdot)$ term in the second to last equality is a bounded quantity.

Note that under H_{1i} , $X_i \sim N(0, 1 + \psi^2)$. Therefore, by (64) and the fact that $\lim_{n \rightarrow \infty} \frac{\psi_n^2}{1 + \psi_n^2} = 1$ (by the second condition of Assumption 1), we have

$$t_{2i} \leq P \left(|Z| < \sqrt{\frac{2}{\eta(1 - \delta)}} \sqrt{\frac{\log(a(\eta\delta)^{-a} b_n^{-1})}{\psi^2}} (1 + o(1)) \right) \text{ as } n \rightarrow \infty. \quad (65)$$

By assumption, $\lim_{n \rightarrow \infty} \frac{b_n^{1/4}}{p_n} \in (0, \infty)$. This then implies that $\lim_{n \rightarrow \infty} \frac{b_n^{7/8}}{p_n^2} = 0$. Therefore, by the fourth condition of Assumption 1 and the fact that $\psi^2 \rightarrow \infty$ as $n \rightarrow \infty$, we have

$$\begin{aligned}
\frac{\log(a(\eta\delta)^{-a} b_n^{-1})}{\psi^2} &= \frac{\log(a(\eta\delta)^{-a}) + \log(b_n^{-1})}{\psi^2} \\
&= \left(\frac{\log(b_n^{-1/8})}{\psi^2} + \frac{\log(b_n^{-7/8})}{\psi^2} \right) (1 + o(1)) \\
&= \frac{\log(b_n^{-1/2})}{4\psi^2} (1 + o(1)) \\
&\rightarrow \frac{C}{4} \text{ as } n \rightarrow \infty. \quad (66)
\end{aligned}$$

Thus, using (65) and (66), we have

$$t_{2i} \leq P \left(|Z| < \sqrt{\frac{C}{2\eta(1 - \delta)}} (1 + o(1)) \right) \text{ as } n \rightarrow \infty$$

$$\begin{aligned}
&= P \left(|Z| < \sqrt{\frac{C}{2\eta(1-\delta)}} \right) (1 + o(1)) \text{ as } n \rightarrow \infty \\
&= 2 \left[\Phi \left(\sqrt{\frac{C}{2\eta(1-\delta)}} \right) - 1 \right] (1 + o(1)) \text{ as } n \rightarrow \infty.
\end{aligned}$$

□

Lemma 6. *Suppose we have the same set-up as Lemma 4. Then a lower bound for the probability of a Type II error for the i th test is given by*

$$t_{2i} \geq \left[2\Phi(\sqrt{C}) - 1 \right] (1 + o(1)) \text{ as } n \rightarrow \infty,$$

where the $o(1)$ terms tend to zero as $n \rightarrow \infty$.

Proof of Lemma 6. By definition, the probability of a Type II error for the i th decision is given by

$$t_{2i} = P \left(\mathbb{E}(1 - \kappa_i) \leq \frac{1}{2} \middle| H_{1i} \text{ is true} \right).$$

For any n , we have by Theorem 2 that

$$\left\{ e^{X_i^2/2} \left(\frac{b_n}{a + b_n + 1/2} \right) \leq \frac{1}{2} \right\} \subseteq \left\{ \mathbb{E}(1 - \kappa_i | X_i) \leq \frac{1}{2} \right\}.$$

Therefore,

$$\begin{aligned}
t_{2i} &= P \left(\mathbb{E}(1 - \kappa_i | X_i) \leq \frac{1}{2} \middle| H_{1i} \text{ is true} \right) \\
&\geq P \left(e^{X_i^2/2} \left(\frac{b_n}{a + b_n + 1/2} \right) \leq \frac{1}{2} \middle| H_{1i} \text{ is true} \right) \\
&= P \left(X_i^2 \leq 2 \log \left(\frac{a + b_n + 1/2}{2b_n} \right) \middle| H_{1i} \text{ is true} \right). \tag{67}
\end{aligned}$$

Since $X_i \sim N(0, 1 + \psi^2)$ under H_{1i} , we have by the second condition in Assumption 1 that $\lim_{n \rightarrow \infty} \frac{\psi_n^2}{1 + \psi_n^2} \rightarrow 1$. From (67) and the facts that $a \in (\frac{1}{2}, \infty)$ and $b_n \in (0, 1)$ for all n (so $b_n^{-1} \geq b_n^{-1/2}$ for all n), we have for sufficiently large n ,

$$t_{2i} \geq P \left(|Z| \leq \sqrt{\frac{2 \log \left(\frac{a + b_n + 1/2}{2b_n} \right)}{\psi^2}} (1 + o(1)) \right) \text{ as } n \rightarrow \infty$$

$$\begin{aligned}
&\geq P\left(|Z| \leq \sqrt{\frac{\log\left(\frac{1}{2b_n}\right)}{\psi^2}(1+o(1))}\right) \text{ as } n \rightarrow \infty \\
&\geq P\left(|Z| \leq \sqrt{\frac{\log(b_n^{-1/2}) + \log(1/2)}{\psi^2}(1+o(1))}\right) \text{ as } n \rightarrow \infty \\
&= P(|Z| \leq \sqrt{C})(1+o(1)) \text{ as } n \rightarrow \infty \\
&= 2[\Phi(\sqrt{C}) - 1](1+o(1)) \text{ as } n \rightarrow \infty,
\end{aligned}$$

where in the second to last equality, we used the assumption that $\lim_{n \rightarrow \infty} \frac{b_n^{1/4}}{p_n} \in (0, \infty)$ and the second and fourth conditions from Assumption 1. \square

Proof of Theorem 8. Since the κ_i 's, $i = 1, \dots, n$ are *a posteriori* independent, the Type I and Type II error probabilities t_{1i} and t_{2i} are the same for every test $i, i = 1, \dots, n$. By Lemmas 3 and 4, for large enough n ,

$$\begin{aligned}
&2 \left(1 - \Phi \left(\sqrt{\frac{2}{\eta(1-\delta)} \left[\log \left(\frac{\left(a + \frac{1}{2}\right)(1-\eta)^{b_n}}{b_n(\eta\delta)^{a+\frac{1}{2}} \left(\frac{1}{2} - \eta\right)} \right) \right]} \right) \right) \leq t_{1i} \\
&\leq \frac{2b_n}{\sqrt{\pi}(a + b_n + 1/2)} \left[\log \left(\frac{a + b_n + 1/2}{2b_n} \right) \right]^{-1/2}.
\end{aligned}$$

Taking the limit as $n \rightarrow \infty$ of all the terms above and using the sandwich theorem, we have

$$\lim_{n \rightarrow \infty} t_{1i} = 0 \quad (68)$$

for the i th test, under the assumptions on the hyperparameters a and b_n .

By Lemmas 5 and 6, for any $\eta \in (0, \frac{1}{2})$ and $\delta \in (0, 1)$,

$$\left[2\Phi(\sqrt{C}) - 1 \right] (1 + o(1)) \leq t_{2i} \leq \left[2\Phi \left(\sqrt{\frac{C}{2\eta(1-\delta)}} \right) - 1 \right] (1 + o(1)). \quad (69)$$

Therefore, we have by (68) and (69) that as $n \rightarrow \infty$, the asymptotic risk (23) of the classification rule (27), R_{IGG} , can be bounded as follows:

$$np(2\Phi(\sqrt{C}) - 1)(1 + o(1)) \leq R_{IGG} \leq np \left(2\Phi \left(\sqrt{\frac{C}{2\eta(1-\delta)}} \right) - 1 \right) (1 + o(1)). \quad (70)$$

Therefore, from (25) and (70), we have as $n \rightarrow \infty$,

$$1 \leq \liminf_{n \rightarrow \infty} \frac{R_{IGG}}{R_{Opt}^{BO}} \leq \limsup_{n \rightarrow \infty} \frac{R_{IGG}}{R_{Opt}^{BO}} \leq \frac{2\Phi\left(\sqrt{\frac{C}{2\eta(1-\delta)}}\right) - 1}{2\Phi(\sqrt{C}) - 1}. \quad (71)$$

Now, the supremum of $\eta(1-\delta)$ over the grid $(\eta, \delta) \in (0, \frac{1}{2}) \times (0, 1)$ is clearly $\frac{1}{2}$, and so the infimum of the numerator in the right-most term in (71) is therefore $2\Phi(\sqrt{C}) - 1$. Thus, one has that

$$1 \leq \liminf_{n \rightarrow \infty} \frac{R_{IGG}}{R_{Opt}^{BO}} \leq \limsup_{n \rightarrow \infty} \frac{R_{IGG}}{R_{Opt}^{BO}} \leq 1,$$

so classification rule (27) is ABOS, i.e.

$$\frac{R_{IGG}}{R_{Opt}^{BO}} \rightarrow 1 \text{ as } n \rightarrow \infty.$$

□

References

- [1] Abramovich, F., Grinshtein, V., and Pensky, M. (2007). On optimality of bayesian testimation in the normal means problem. *Ann. Statist.*, 35(5):2261–2286.
- [2] Armagan, A., Clyde, M., and Dunson, D. B. (2011). Generalized beta mixtures of gaussians. In Shawe-taylor, J., Zemel, R., Bartlett, P., Pereira, F., and Weinberger, K., editors, *Advances in Neural Information Processing Systems 24*, pages 523–531.
- [3] Armagan, A., Dunson, D. B., and Lee, J. (2013). Generalized double pareto shrinkage. *Statistica Sinica*, 23 1:119–143.
- [4] Benjamini, Y. and Hochberg, Y. (1995). Controlling the false discovery rate: A practical and powerful approach to multiple testing. *Journal of the Royal Statistical Society. Series B (Methodological)*, 57(1):289–300.
- [5] Berger, J. (1980). A robust generalized bayes estimator and confidence region for a multivariate normal mean. *Ann. Statist.*, 8(4):716–761.
- [6] Bhadra, A., Datta, J., Polson, N. G., and Willard, B. (2017). The horseshoe+ estimator of ultra-sparse signals. Advance publication.

- [7] Bhattacharya, A., Pati, D., Pillai, N. S., and Dunson, D. B. (2015). Dirichlet–laplace priors for optimal shrinkage. *Journal of the American Statistical Association*, 110(512):1479–1490. PMID: 27019543.
- [8] Bogdan, M., Chakrabarti, A., Frommlet, F., and Ghosh, J. K. (2011). Asymptotic bayes-optimality under sparsity of some multiple testing procedures. *Ann. Statist.*, 39(3):1551–1579.
- [9] Carvalho, C. M., Polson, N. G., and Scott, J. G. (2009). Handling sparsity via the horseshoe. In van Dyk, D. and Welling, M., editors, *Proceedings of the Twelfth International Conference on Artificial Intelligence and Statistics*, volume 5 of *Proceedings of Machine Learning Research*, pages 73–80, Hilton Clearwater Beach Resort, Clearwater Beach, Florida USA. PMLR.
- [10] Carvalho, C. M., Polson, N. G., and Scott, J. G. (2010). The horseshoe estimator for sparse signals. *Biometrika*, 97(2):465–480.
- [11] Castillo, I. and van der Vaart, A. (2012). Needles and straw in a haystack: Posterior concentration for possibly sparse sequences. *Ann. Statist.*, 40(4):2069–2101.
- [12] Datta, J. and Ghosh, J. K. (2013). Asymptotic properties of bayes risk for the horseshoe prior. *Bayesian Anal.*, 8(1):111–132.
- [13] Donoho, D. L., Johnstone, I. M., Hoch, J. C., and Stern, A. S. (1992). Maximum entropy and the nearly black object. *Journal of the Royal Statistical Society. Series B (Methodological)*, 54(1):41–81.
- [14] George, E. I. and Foster, D. P. (2000). Calibration and empirical bayes variable selection. *Biometrika*, 87(4):731–747.
- [15] George, E. I. and McCulloch, R. E. (1993). Variable selection via gibbs sampling. *Journal of the American Statistical Association*, 88(423):881–889.
- [16] Ghosal, S., Ghosh, J. K., and van der Vaart, A. W. (2000). Convergence rates of posterior distributions. *Ann. Statist.*, 28(2):500–531.
- [17] Ghosh, P. and Chakrabarti, A. (2017). Asymptotic optimality of one-group shrinkage priors in sparse high-dimensional problems. Advance publication.

- [18] Ghosh, P., Tang, X., Ghosh, M., and Chakrabarti, A. (2016). Asymptotic properties of bayes risk of a general class of shrinkage priors in multiple hypothesis testing under sparsity. *Bayesian Anal.*, 11(3):753–796.
- [19] Griffin, J. E. and Brown, P. J. (2013). Some priors for sparse regression modelling. *Bayesian Anal.*, 8(3):691–702.
- [20] Johnstone, I. and Silverman, B. (2005a). Ebayesthresh: R programs for empirical bayes thresholding. *Journal of Statistical Software, Articles*, 12(8):1–38.
- [21] Johnstone, I. M. and Silverman, B. W. (2004). Needles and straw in haystacks: Empirical bayes estimates of possibly sparse sequences. *Ann. Statist.*, 32(4):1594–1649.
- [22] Johnstone, I. M. and Silverman, B. W. (2005b). Empirical bayes selection of wavelet thresholds. *Ann. Statist.*, 33(4):1700–1752.
- [23] Mitchell, T. and Beauchamp, J. (1988). Bayesian variable selection in linear regression. *Journal of the American Statistical Association*, 83(404):1023–1032.
- [24] Park, T. and Casella, G. (2008). The bayesian lasso. *Journal of the American Statistical Association*, 103(482):681–686.
- [25] Ročková, V. (2017). Bayesian estimation of sparse signals with a continuous spike-and-slab prior. *Ann. Statist.* To appear.
- [26] Ročková, V. and George, E. I. (2016). The spike-and-slab lasso. *Journal of the American Statistical Association*, 0(ja):0–0.
- [27] Strawderman, W. E. (1971). Proper bayes minimax estimators of the multivariate normal mean. *Ann. Math. Statist.*, 42(1):385–388.
- [28] Tibshirani, R. (1996). Regression shrinkage and selection via the lasso. *Journal of the Royal Statistical Society, Series B*, 58:267–288.
- [29] Tibshirani, R., Saunders, M., Rosset, S., Zhu, J., and Knight, K. (2005). Sparsity and smoothness via the fused lasso. *Journal of the Royal Statistical Society Series B*, pages 91–108.
- [30] van der Pas, S., Salomond, J.-B., and Schmidt-Hieber, J. (2016). Conditions for posterior contraction in the sparse normal means problem. *Electron. J. Statist.*, 10(1):976–1000.

- [31] van der Pas, S., Szabó, B., and van der Vaart, A. (2017). Uncertainty quantification for the horseshoe. Advance publication.
- [32] van der Pas, S. L., Kleijn, B. J. K., and van der Vaart, A. W. (2014). The horseshoe estimator: Posterior concentration around nearly black vectors. *Electron. J. Statist.*, 8(2):2585–2618.
- [33] Wellcome Trust (2007). Genome-wide association study of 14,000 cases of seven common diseases and 3000 shared controls. *Nature*, 447:661–678.
- [34] Yuan, M. and Lin, Y. (2006). Model selection and estimation in regression with grouped variables. *Journal of the Royal Statistical Society: Series B (Statistical Methodology)*, 68(1):49–67.
- [35] Zou, H. (2006). The adaptive lasso and its oracle properties. *Journal of the American Statistical Association*, 101(476):1418–1429.
- [36] Zou, H. and Hastie, T. (2005). Regularization and variable selection via the elastic net. *Journal of the Royal Statistical Society: Series B (Statistical Methodology)*, 67(2):301–320.